

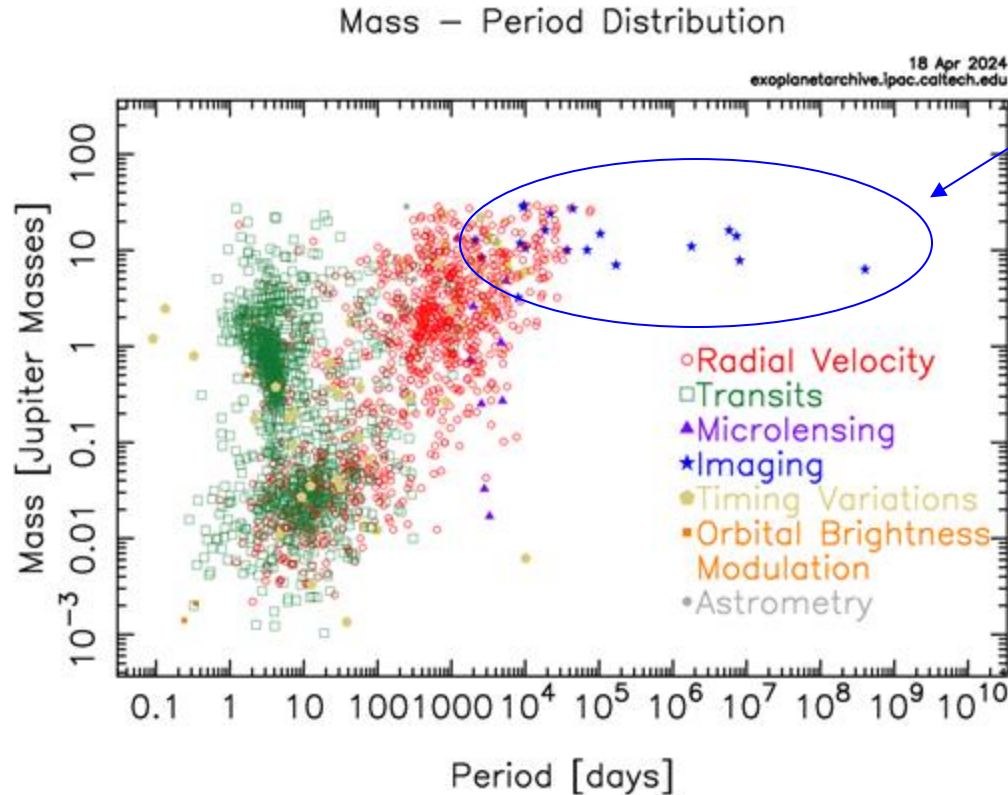


Constraining The Formation And Orbital Architectures of Directly Imaged Exoplanets

Clarissa R. Do Ó (UCSD; NSF Graduate Fellow and San Diego Fellow)
Advisor: Prof. Quinn M. Konopacky (UCSD)

ExoPAG 31 (Jan 11th, 2025)

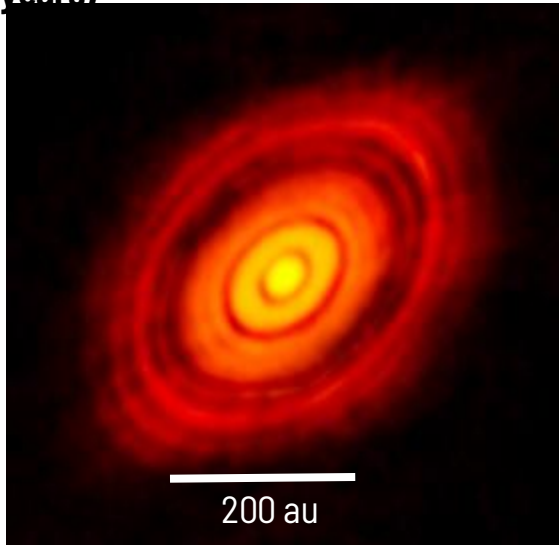
Exoplanet Discoveries So far...



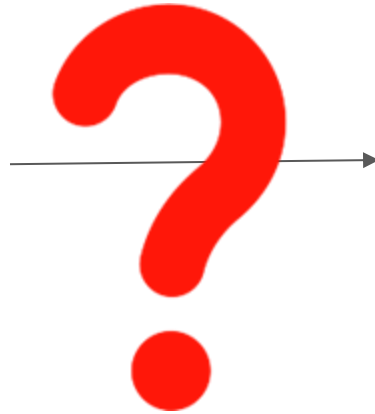
All young, self-luminous, and widely separated gas giants (for now...)

How do exoplanet systems form?

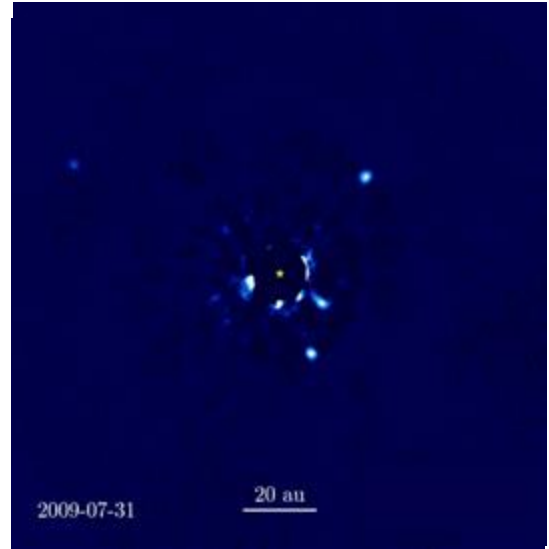
Protoplanetary Disk (**Age ~ 100,000 years**)



Credit: ALMA, C. Brogan, B. Saxton
HL Tau System



Planetary System (**Age ~ 30 million years**)

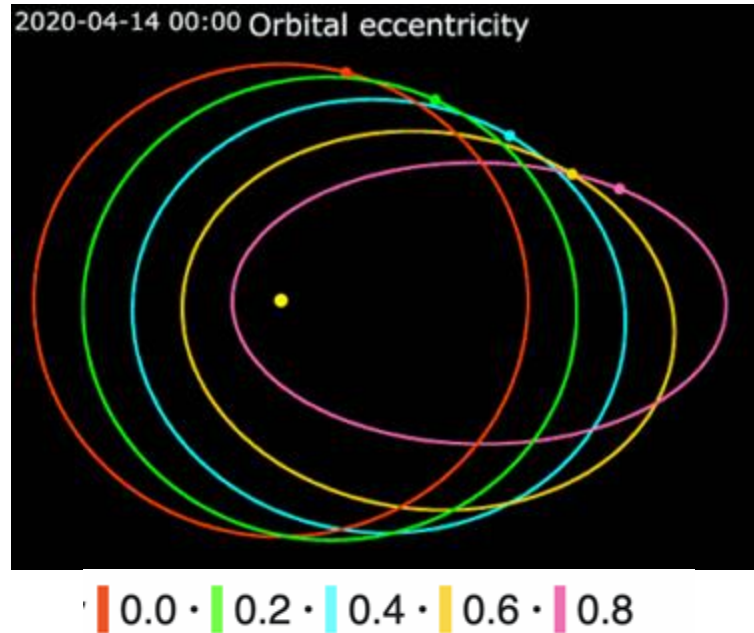


Credit: Jason Wang (Northwestern)/William Thompson (UVic)/Christian Marois (NRC Herzberg)/Quinn Konopacky (UCSD)

HR 8799 System

Exoplanet Orbits & Formation

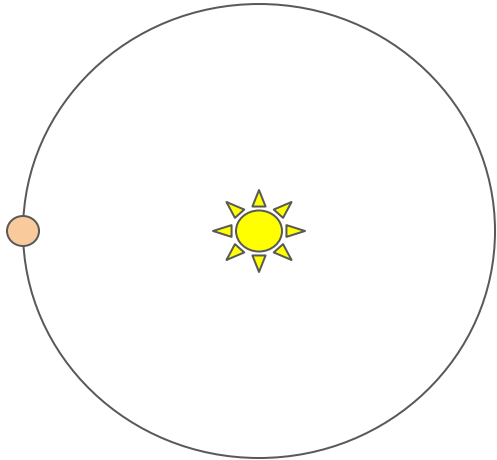
- Orbital parameters of planets can tell us the history on how they were formed
- The **eccentricity** of the planet is of particular interest



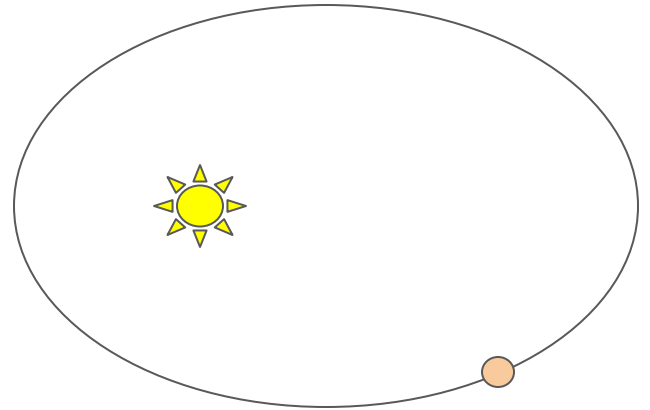
Credit: Wikipedia

Planets form from protoplanetary disks...

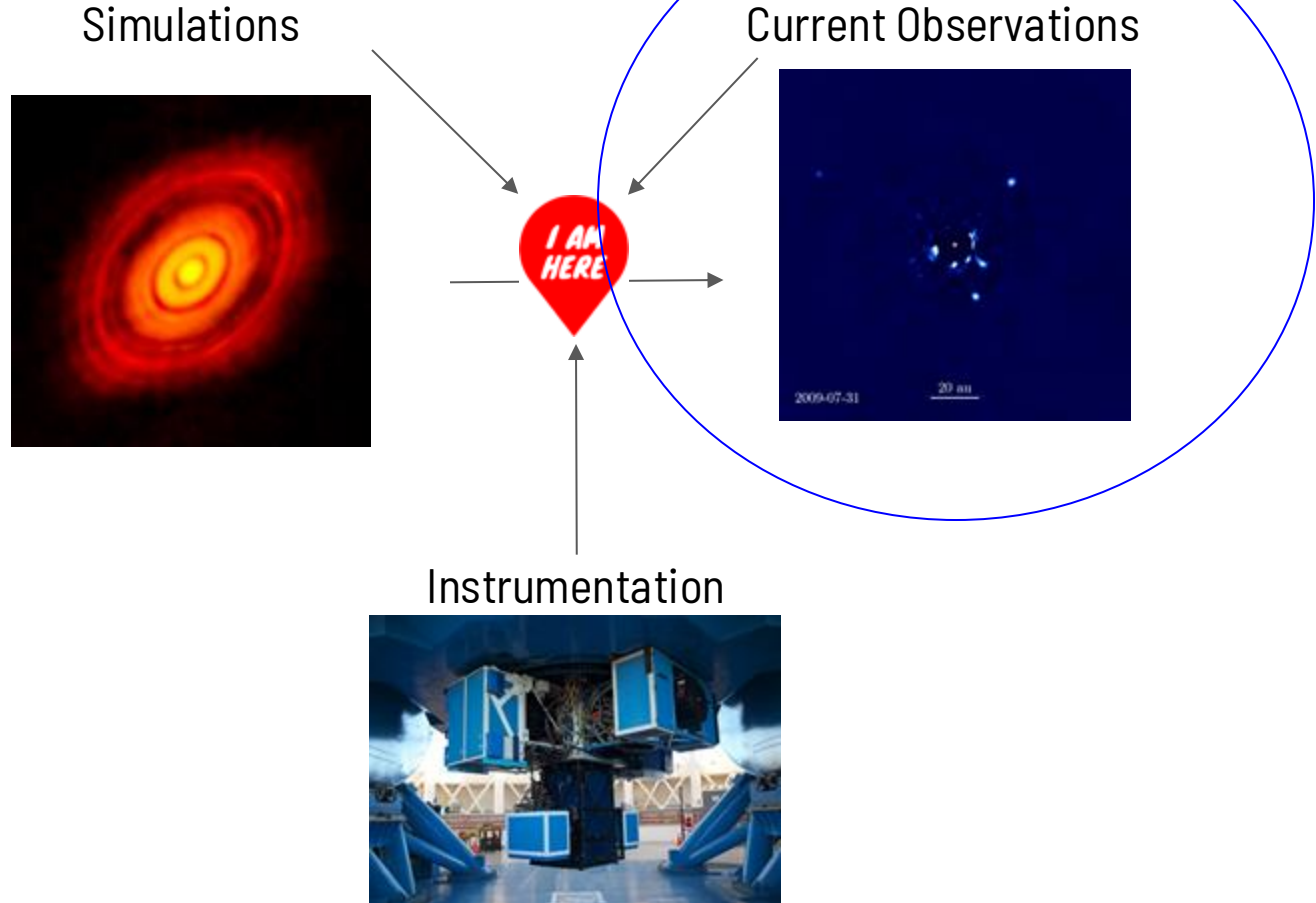
- **Core Accretion:** gas giant slowly forms in disk
 - **Orbits expected to be near-circular ($e < 0.2$)**



- **Gravitational Instability:** gas giant rapidly forms in disk
 - **Could potentially form planets with more elliptical orbits ($e > 0.2$)**



Many tools to answer one question...



Population-Level Eccentricities of Exoplanets and Brown Dwarfs Using Observable Priors

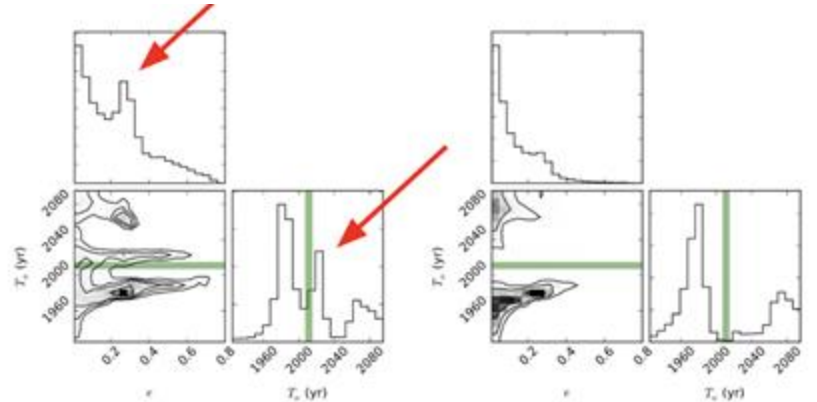
- Do exoplanets ($M < 13 \text{ Mj}$) & brown dwarfs ($13 \text{ Mj} < M < 80 \text{ Mj}$) **have similar or different formation processes?** -> need to look at their eccentricities at population level (e.g. Kipping 2013, Bowler et al 2020)
- Most orbit fits only use relative astrometry (planet-star position over time) to fit for orbits -> **because of long periods, data is undersampled**
- **Uniform priors + Undersampling of data -> Biases in orbital parameters (O'Neil et al 2019)**

(x, y, t)

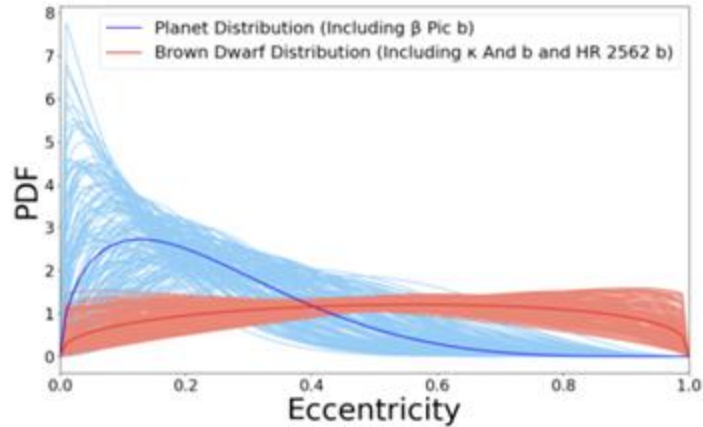
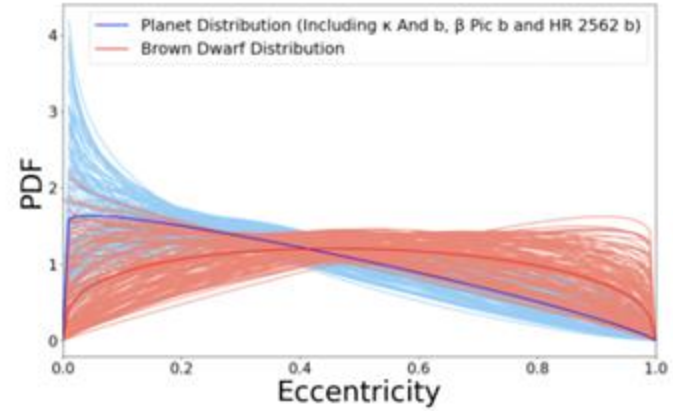
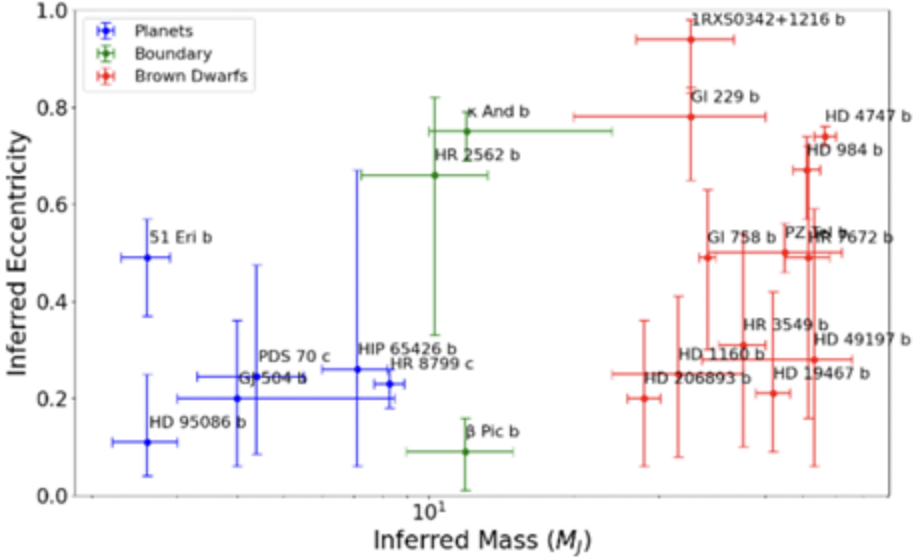
(x', y', t')



(O'Neil et al 2019)

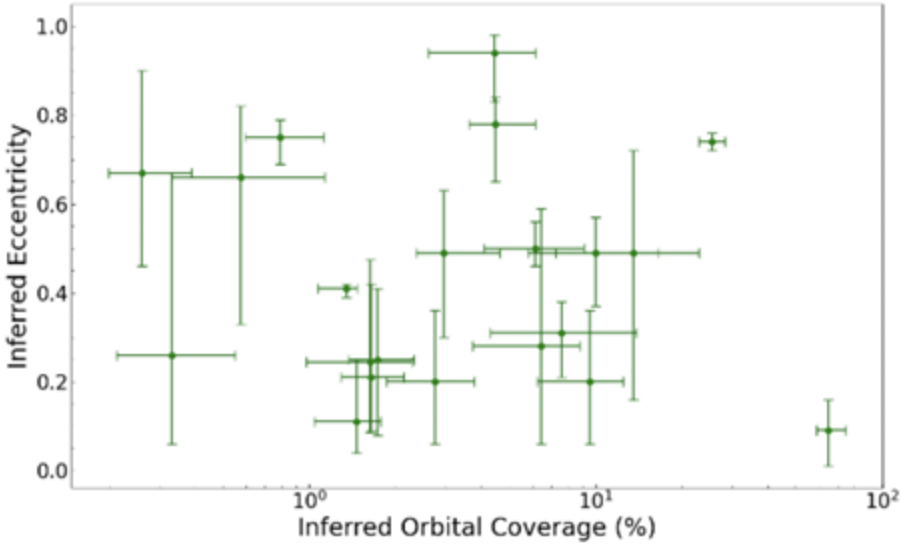


Population-Level Eccentricities of Exoplanets and Brown Dwarfs Using Observable Priors

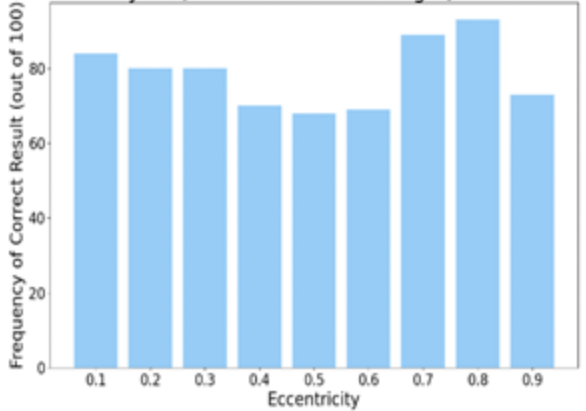


(Do Ó et al. 2023a, AJ)

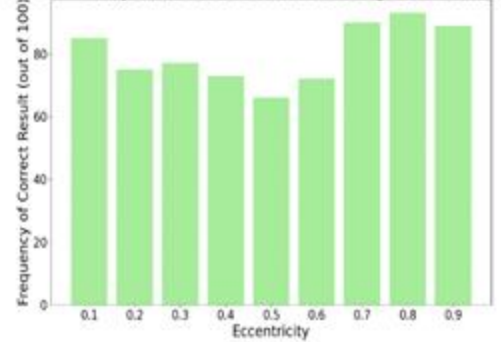
Found that we need additional Orbital Coverage + more than relative astrometry alone...



Period = 200 years, 15% of Orbital Coverage (Observable Priors)



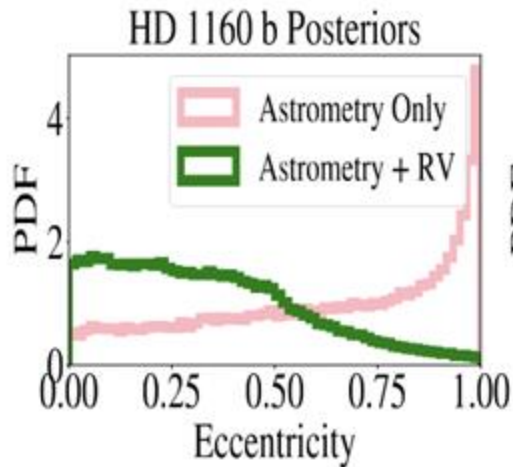
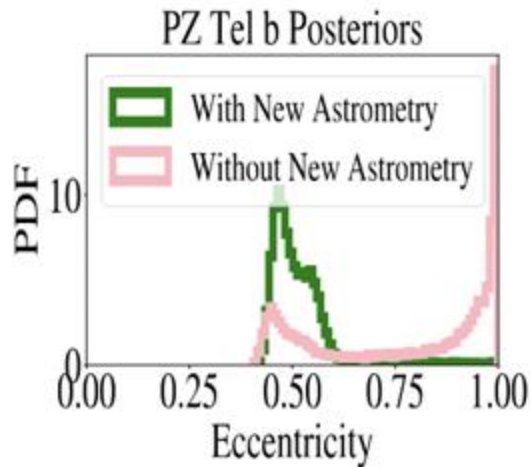
Period = 200 years, 15% of Orbital Coverage (Uniform Priors)



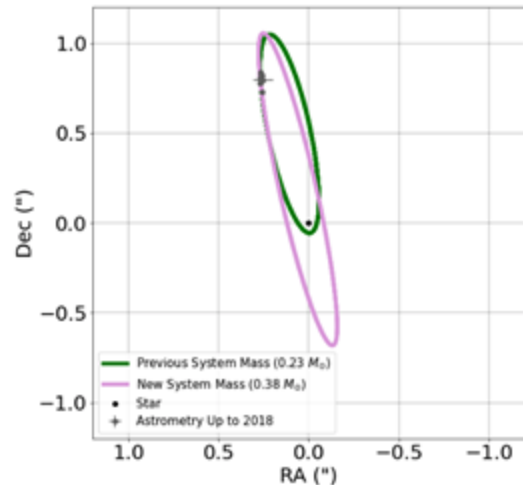
(Do Ó et al. 2023a, AJ)

Average coverage ~ 7.4%

Significant Changes in Orbital Posteriors with New Astrometry and RV Data from Keck/NIRC2 and Keck/KPIC

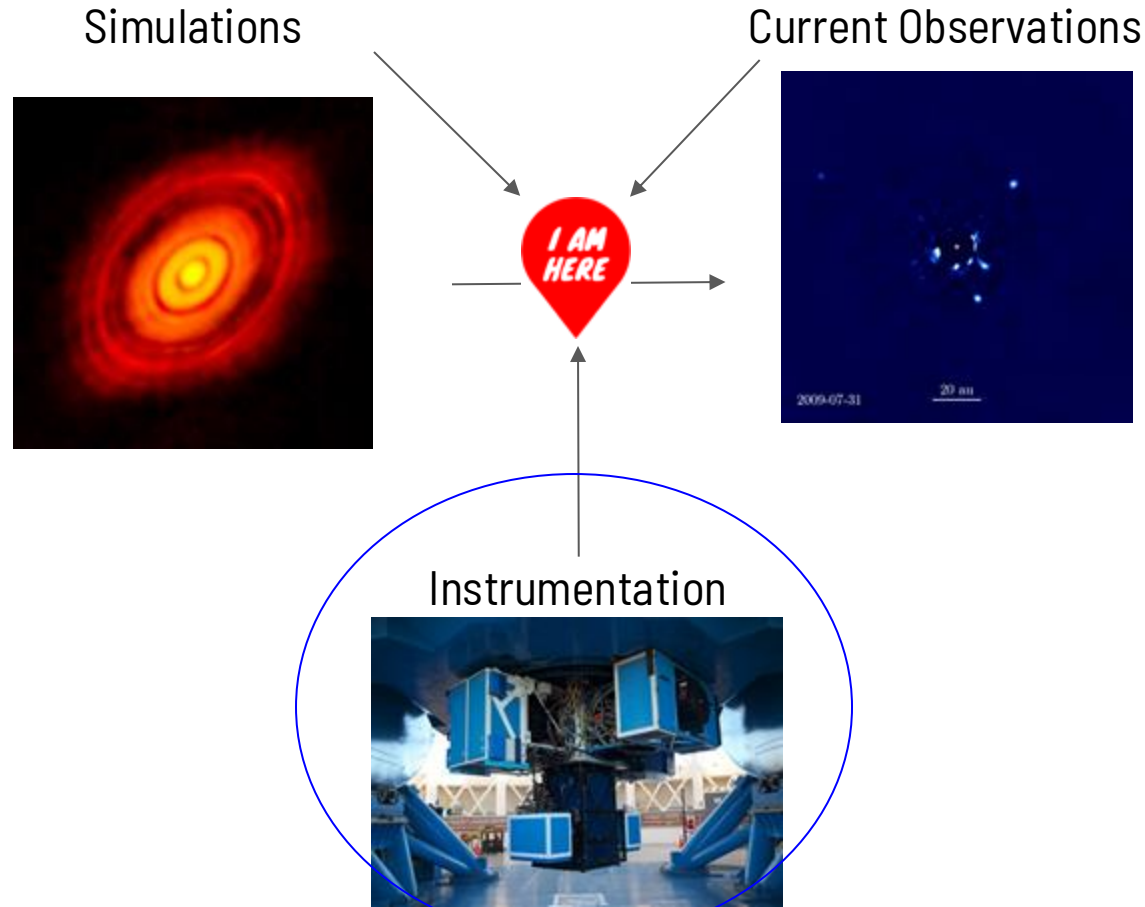


(Do Ó et al. 2023a, AJ)



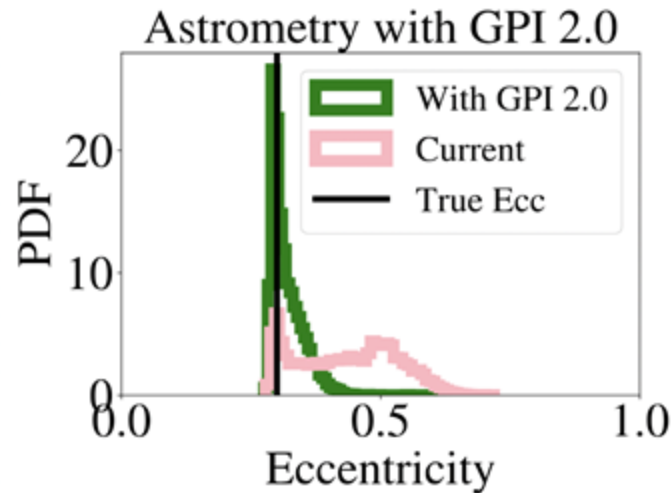
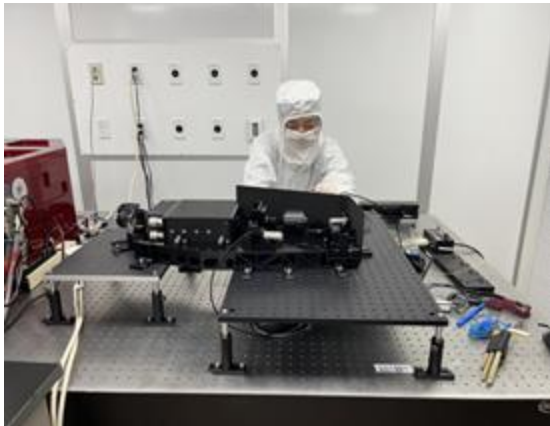
1RXS 0342 + 1216 b (Do Ó et al. 2024a, AJ)

Many tools to answer one question...



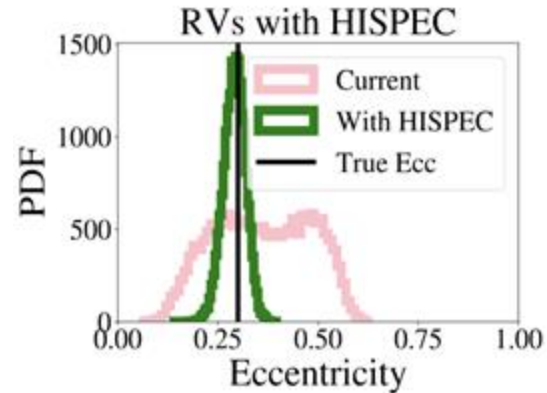
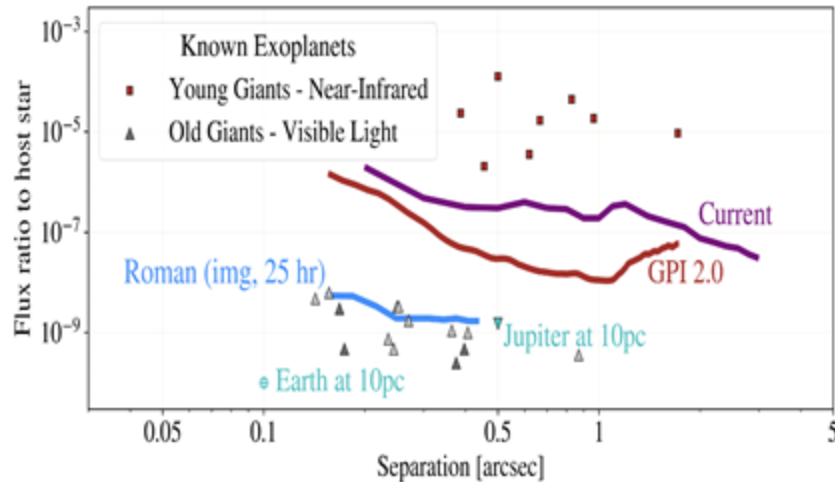
Improved Astrometry (and detection limits) will come from the Gemini Planet Imager 2.0 (GPI 2.0)

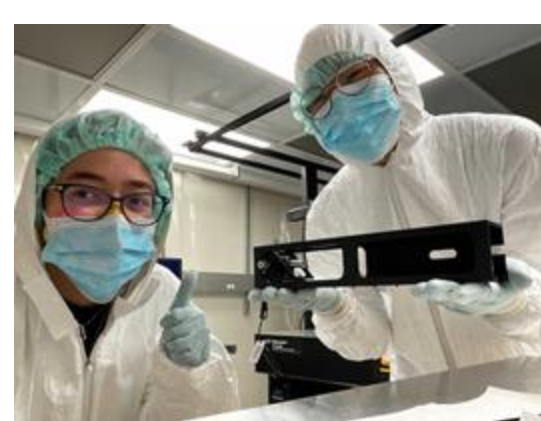
- Upgrades to several subsystems will lead to an improvement in contrast by a factor of ~ 10 and astrometry by a factor of 5 (Chilcote et al 2018)
- I contributed to its wavefront sensor upgrade (from Shack-Hartmann to Pyramid) at UCSD
 - Tested its EMCCD camera (Do Ó et al 2023b and Do Ó et al 2024b)
 - Aligned its telescope simulator
 - Operation will be at 2 kHz



The path to finding complete orbital architectures of systems...

- Gaia DR4 (2026) - dynamical masses + more targets to look at
- HISPEC (2026) - EPRVs of Exoplanets
- Roman Coronagraph (2027) - image old gas giants in reflected light
- Habitable Worlds Observatory (2040s) - image inner planets, including exo-Earths!



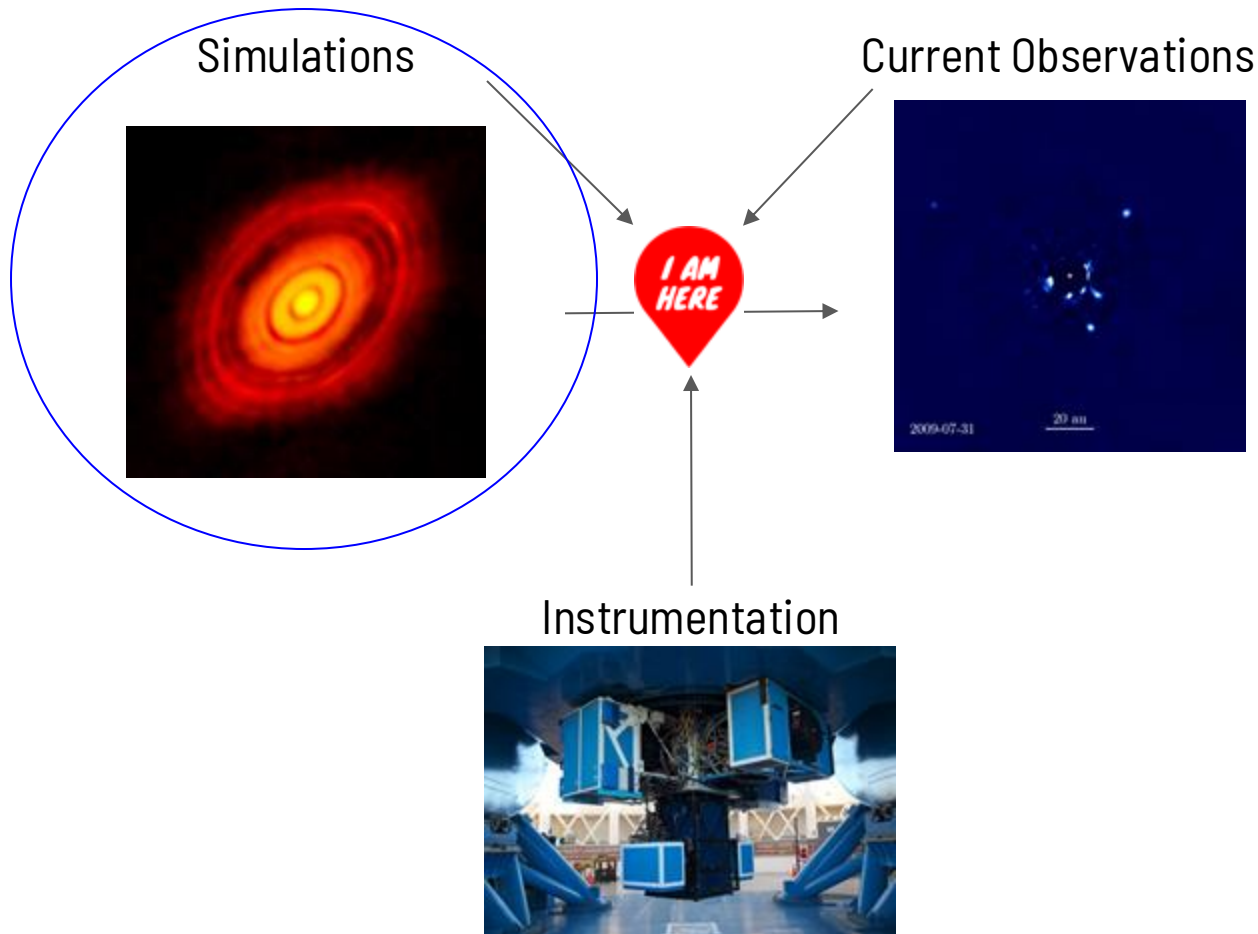


Thank you! Questions?

clarissardoo.github.io || cdoos@ucsd.edu

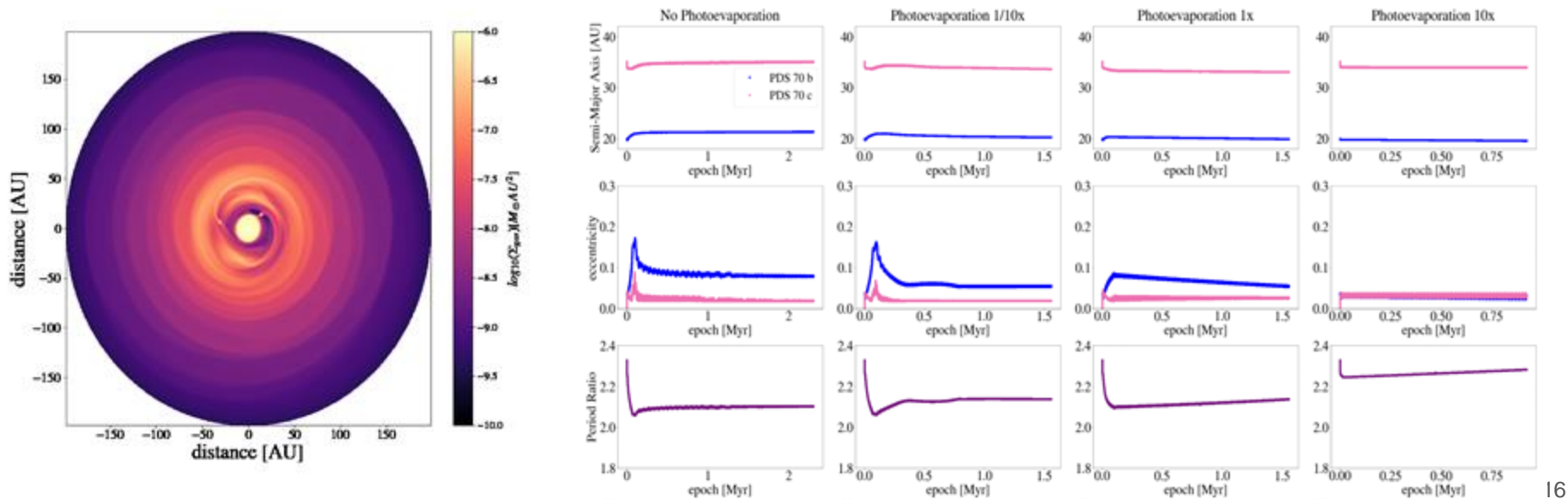


Many tools to answer one question...



More comparisons with theoretical models on eccentricity expectations... (Do Ó et al in prep)

- Performing hydrodynamic simulations on PDS 70 system (two protoplanets embedded in the protoplanetary disk) including disk photoevaporation for the first time
- Will perform N-body simulations once the disk is fully evaporated



Recovering Population Distribution

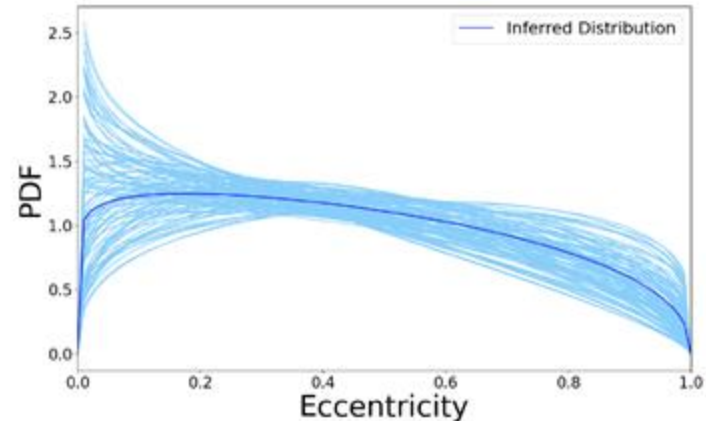
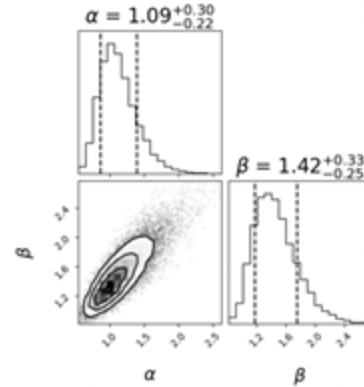
(Do Ó et al. 2023)

Can use a Beta Distribution (Bowler et al. 2020, Hogg et al. 2010, Kipping 2013) as a model for the eccentricity distribution:

$$f(e, \alpha, \beta) = \frac{\Gamma(\alpha + \beta)e^{\alpha-1}(1 - e)^{\beta-1}}{\Gamma(\alpha)\Gamma(\beta)}$$

\

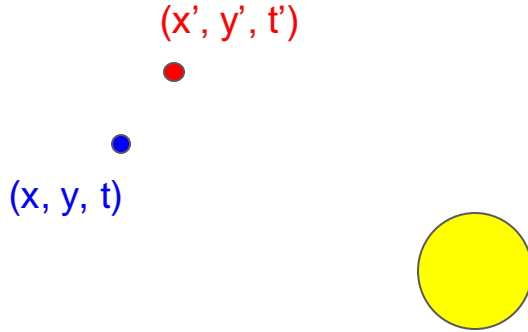
- Governed by two parameters: α and β
- can take many shapes depending on α and β values
- Fit for α and β using eccentricity posteriors from sample



Significant Changes in Orbital Posteriors (New Priors)

- HD 49197 b: $0.62^{+0.33}_{-0.43}$ to $0.28^{+0.29}_{-0.20}$
- HR 2562 b: $0.49^{+0.44}_{-0.36}$ to $0.66^{+0.16}_{-0.33}$
- HIP 65426 b: $0.57^{+0.29}_{-0.38}$ to $0.26^{+0.41}_{-0.20}$

Positions to Parameters...?



Eccentric Anomaly

$$E - e \sin E = 2\pi/P (t - T_0)$$

$$x = BX + GY$$

$$y = AX + FY$$

$$z = CX + HY$$

Geometrical Elements

$$A = a [\cos\Omega \cos\omega - \sin\Omega \sin\omega \cos i]$$

$$B = a [\sin\Omega \cos\omega + \cos\Omega \sin\omega \cos i]$$

$$C = a [\sin\omega \sin(i)]$$

$$F = a [-\cos\Omega \sin\omega - \sin\Omega \cos\omega \cos i]$$

$$G = a [-\sin\Omega \sin\omega + \cos\Omega \cos\omega \cos i]$$

$$H = a [\cos\omega \sin(i)]$$


Dynamical Elements/Observables

$$X = \cos E - e$$

$$Y = (1 - e^2)^{1/2} \sin E$$

Jeffreys Prior v. Observable prior

Observable priors (general form)

$$\mathcal{P}(\mathcal{M}|t) = \mathcal{P}(\mathcal{O}|t) \left| \frac{\partial(\mathcal{O}(t))}{\partial(\mathcal{M})} \right|$$
$$\propto \frac{1}{\prod_i \sigma_i(t)} \left| \frac{\partial(\mathcal{O}(t))}{\partial(\mathcal{M})} \right|,$$


Inversely proportional to measurement uncertainty so different weight on measured observables

Different idea: Rather than being based on the abstract concept of information content, the observable-based prior is based on the practical idea that there should be an equal probability of obtaining observations in regions of parameter-space that are possible to observe. (O'Neil et al. 2019)

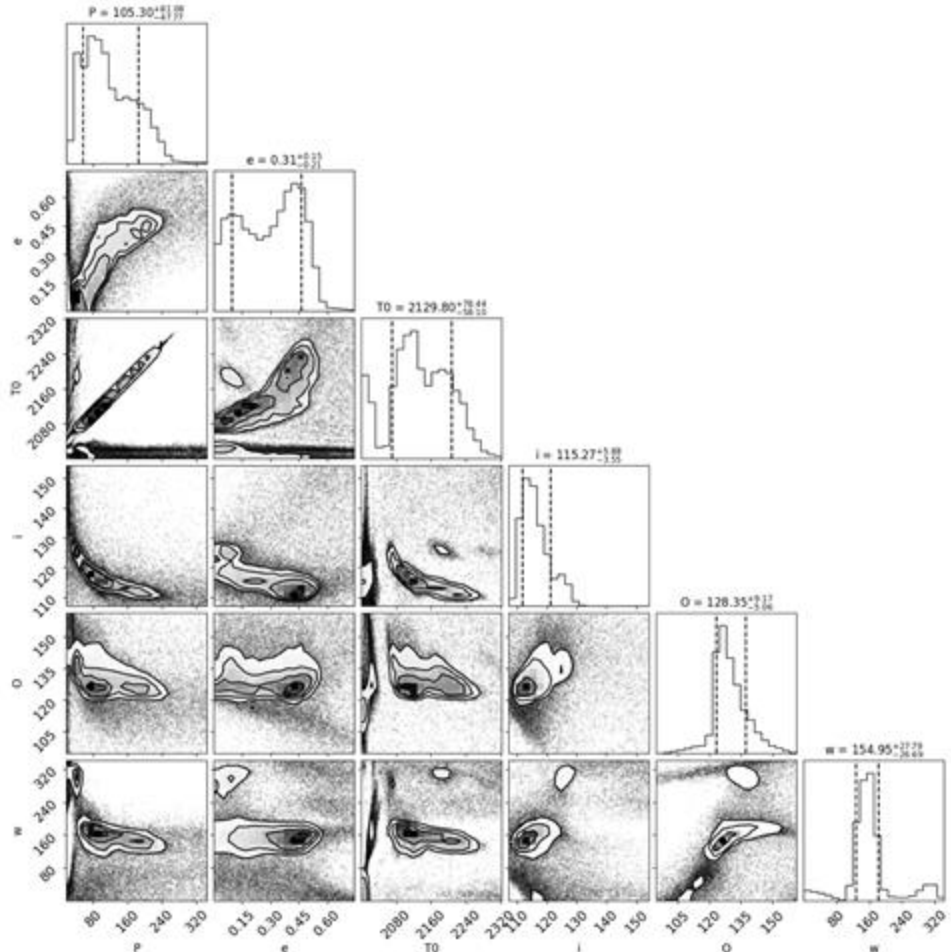
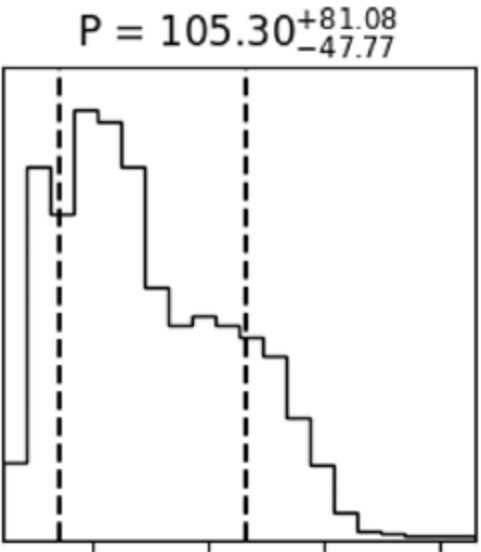
Orbital Observables & Priors (O'Neil et al 2019)

$$\mathcal{P}(P, e) \propto \left\{ \begin{array}{l} \sum_i \frac{1}{R_o^2 \sigma_x(t_i) \sigma_y(t_i)} |J_{\text{astro}}(t_i)| \\ \sum_i \frac{1}{R_o^2 \sigma_x(t_i) \sigma_y(t_i)} |J_{\text{astro}}(t_i)| + \sum_j \frac{1}{\sigma_{v_z}^2(t_j)} |J_{\text{RV}}(t_j)| \end{array} \right.$$

$$J_{\text{astro}} \equiv \frac{\partial(X, Y)}{\partial(e, P)} = - \left(\frac{(GM)^2 P}{2\pi^4} \right)^{1/3} \\ \times \frac{[2(e^2 - 2) \sin E + e(3m + \sin 2E) + 3m \cos E]}{6 \sqrt{1 - e^2}}.$$

$$\sigma_X \sigma_Y = \frac{R_o^2}{\begin{vmatrix} B & G \\ A & F \end{vmatrix}} \sigma_x \sigma_y = f(\Omega, \omega, i) R_o^2 \sigma_x \sigma_y,$$

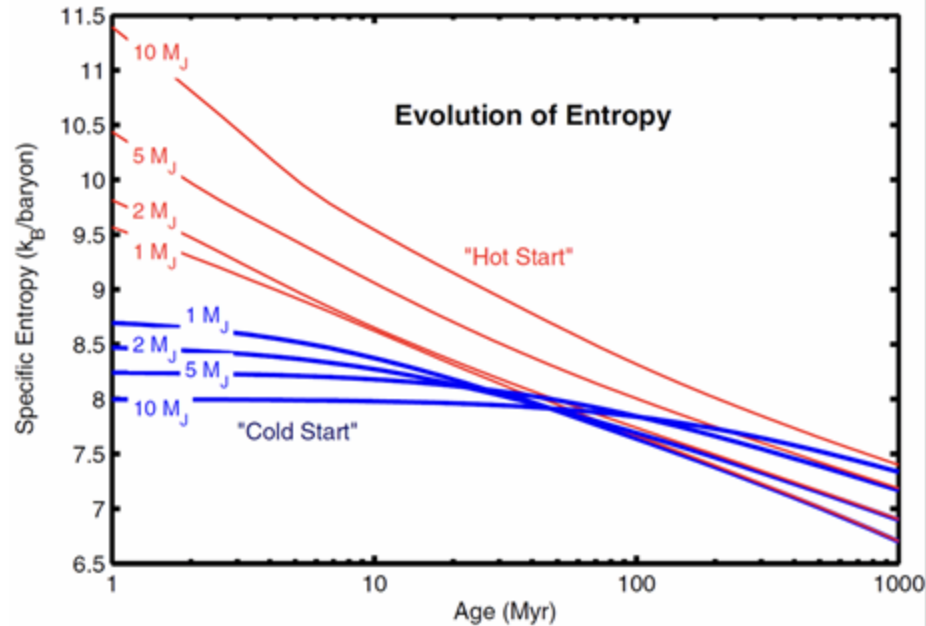
Example Corner Plot: HD 984 B



The image shows a large industrial facility, likely a particle accelerator or a large-scale scientific instrument. The structure is composed of a complex white lattice of beams and supports, forming a large, curved, dome-like structure. In the foreground, there is a large blue machine with multiple levels and platforms, possibly a detector or a component of the instrument. The floor is a light-colored, polished surface. The overall scene is brightly lit, suggesting an indoor environment with large windows or skylights.

Instrumentation Approach

Formation & Entropy (Spiegel & Burrows 2012)

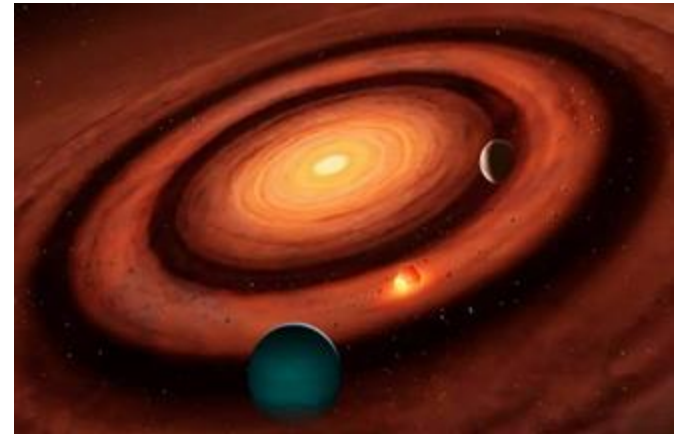
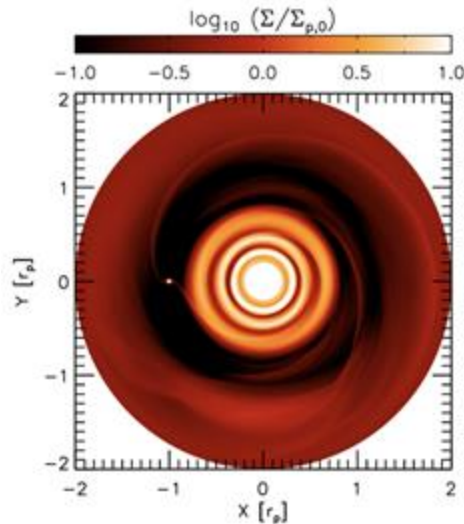


Core accretion: the solid core accretes gas through an accretion disk. This **process cools the gas, causing it to lose much of its initial entropy** and forms a giant planet that has low initial entropy

Gravitational Instability: the gas that collapses directly to form a giant planet retains most of its initial entropy, resulting in high initial entropy (i.e. a "hot-start").

Planets form from protoplanetary disks...

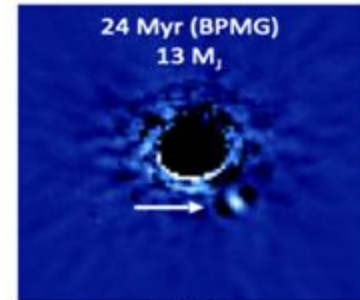
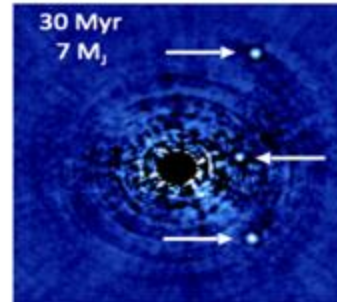
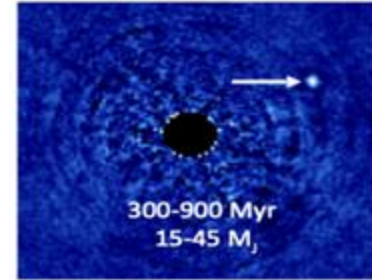
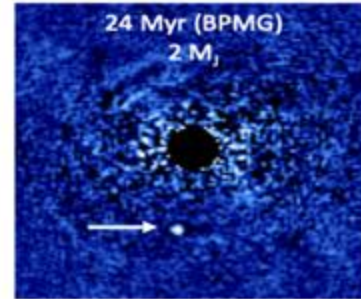
- **Core Accretion:** gas giant slowly forms in disk
 - Timescales: 1 - 10 Myr (Pollack et al 1996)
- **Gravitational Instability:** gas giant rapidly forms in disk
 - Timescales: 10,000 - 100,000 years (Boss 1997)



Credit: Jaehan Bae and MPIA

Gemini Planet Imager (GPI) 1.0

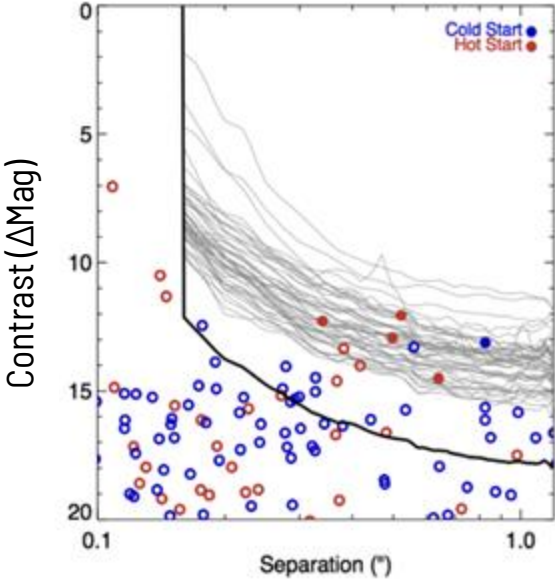
- The Gemini Planet Imager is a **high contrast imaging** instrument
- Operated for 6 years on the Gemini South Observatory
- **Directly images and characterizes Jupiter-mass exoplanets in wide orbits**
- Decommissioned in August 2020 for upgrades
- Will be moved to Gemini North



GPI 1.0 → GPI 2.0

- Science Goal: Achieve higher contrast to find Jupiter-like planets **closer to their stars** and consistent with “cold start” formation models

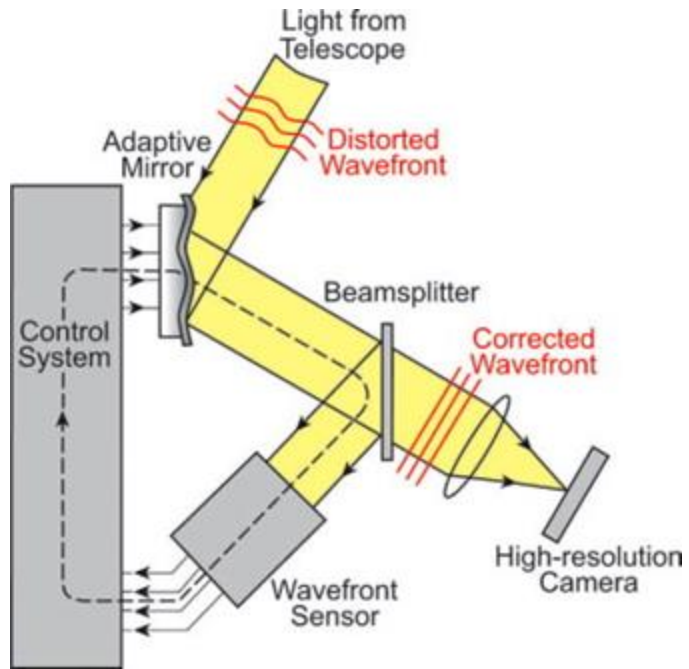
$$mag_{planet} - mag_{star} = -2.5 \log_{10} (F_{planet} / F_{star})$$



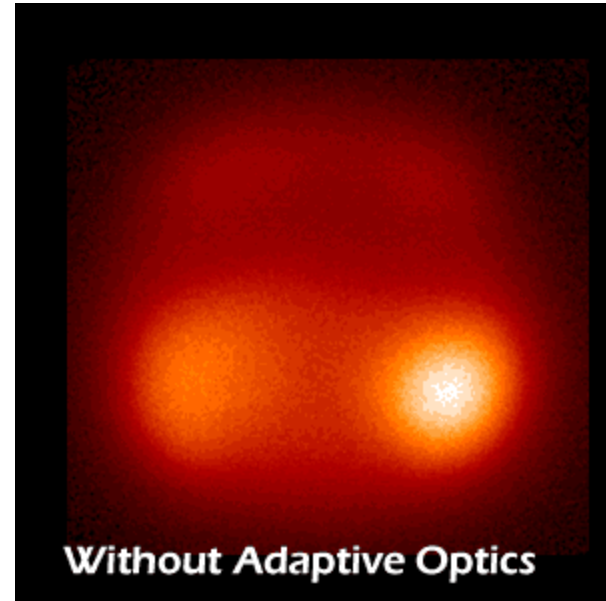
Credit: Chilcote et al. 2018

Science Goals	WFS I-magnitude	Inner working Angle	Contrast Improvements
Large-scale survey / cold-start planets	10	0.15''	2+ mag
Very young stars + transitional disks	13	0.1''	0
Asteroids & solar system objects	13-14	-	0
Debris Disks	9	0.2''	0
Planet Variability & abundance characterisation	6	0.2''	1% photometry high-res
Evolved Stars	9	0.1''	0
Nearby AGN	14	-	Only modest contrast required

Adaptive Optics



Credit: ScienceDirect

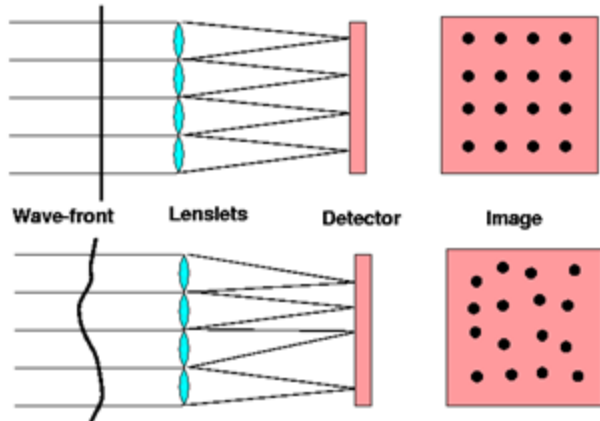


Credit: ESO

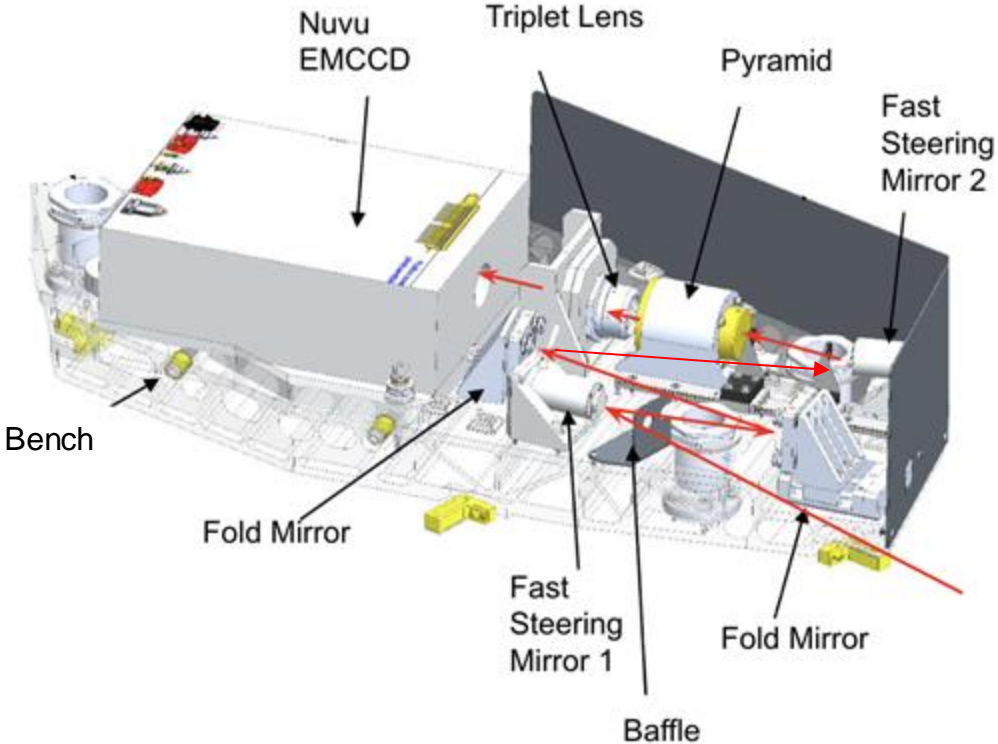
Pyramid Wavefront Sensor Upgrade

Shack-Hartmann Wavefront Sensor (GPI 1.0)

- Lenslet array receives a tilted wavefront and the spot is shifted.
- Measuring the spot displacement enables to derive the wavefront error



Pyramid Wavefront Sensor Upgrade (HAA)

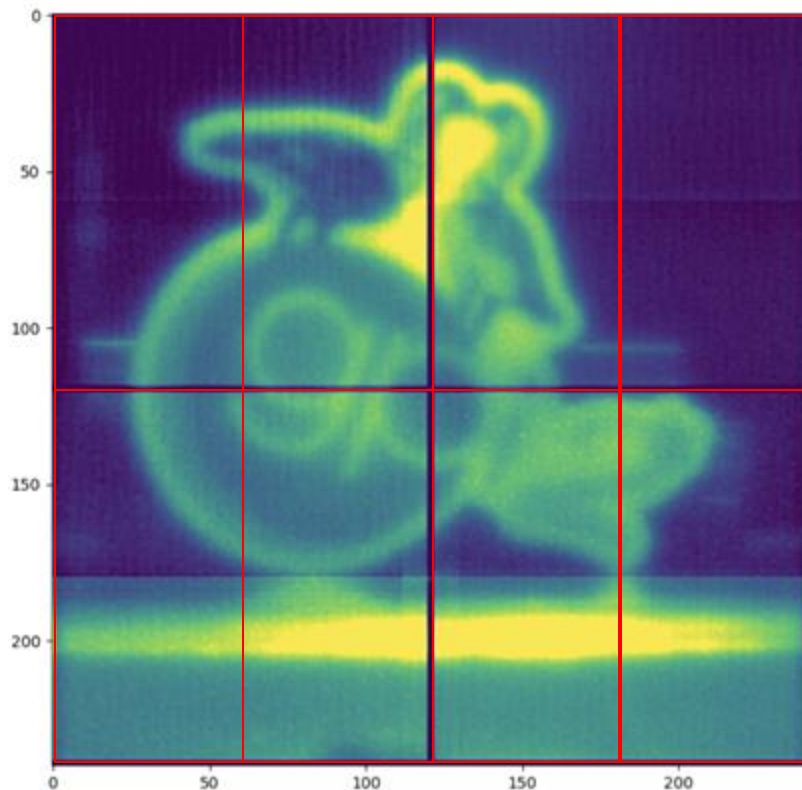


The EMCCD

The EMCCD overview:

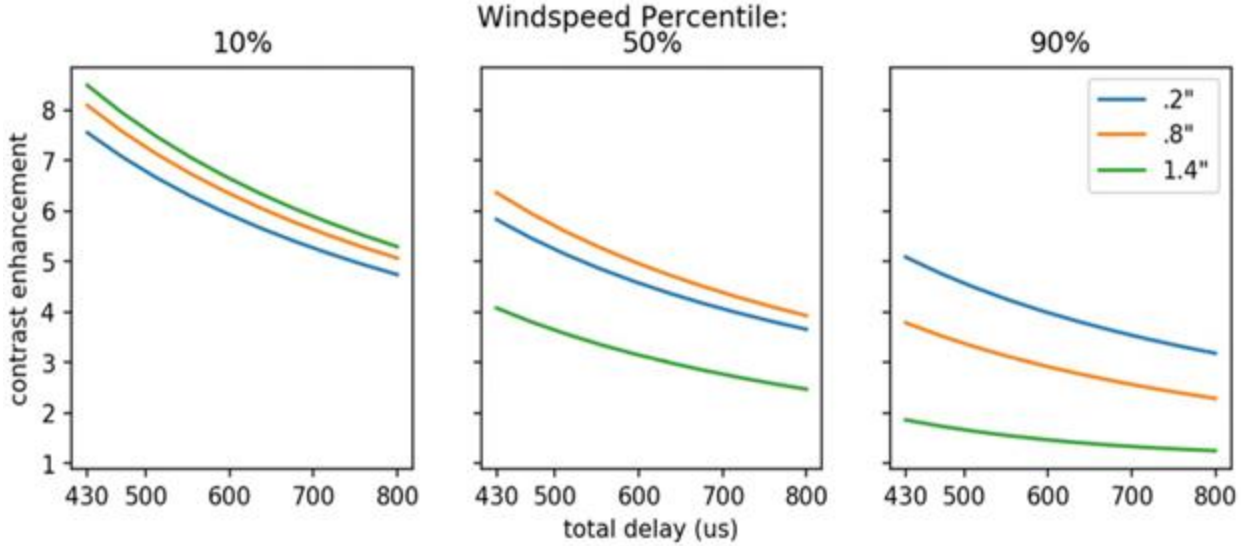
- **Electron multiplying CCDs (EMCCDs)** are detectors capable of counting single photon events at high speed and high sensitivity.
- **8 outputs**
- Operates at 2 kHz (max 3kHz)
- Operates at $-45\text{ }^{\circ}\text{C}$

(Do Ó et al. in prep)



The EMCCD: Motivation

- The delay is the camera readout time + real time control (RTC).
- For GPI 2.0, the aim is to have the RTC at 100 μ s, such that the camera readout dominates the delay.
- EMCCD has a fast readout time



Credit: Madurowicz et al 2020

Current Instrument Status

Preparing GPI for shipping at Gemini South



Going down the mountain



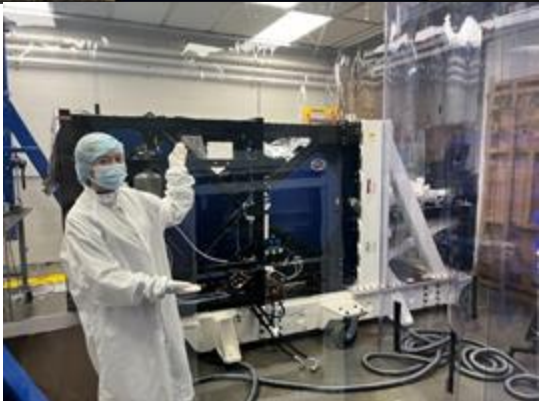
In Transit



Arriving in Notre Dame



Unloaded



In the lab!

Wavefront Sensor Upgrade Status

- Status: integrating at University of Notre Dame
- Checking alignment post-shipment

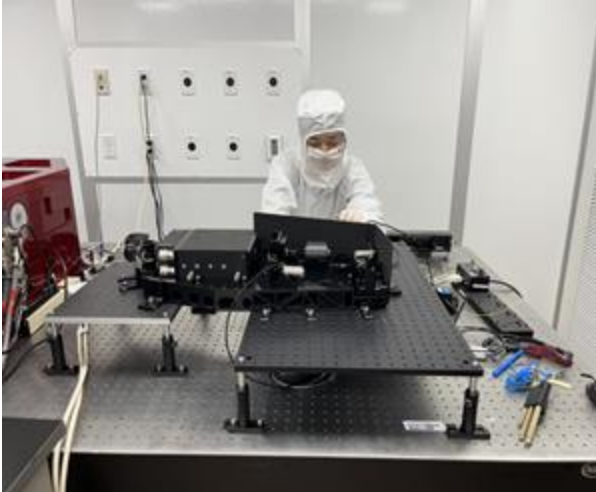


Image Quality Tests

- Camera was not focusing pupils as expected – noticed when we started aligning
- Charge Diffusion issue was causing blurred images that would severely impact our ability to measure the wavefront

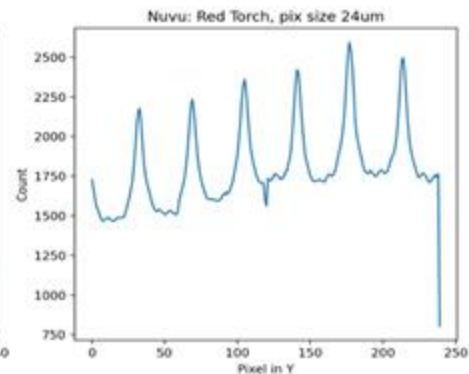
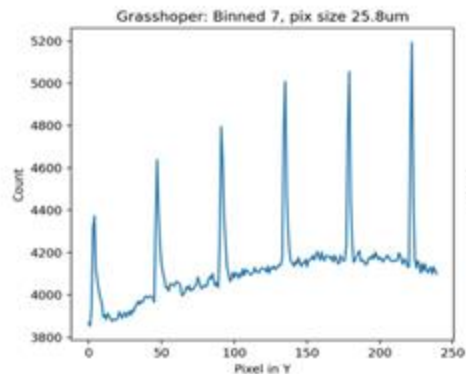
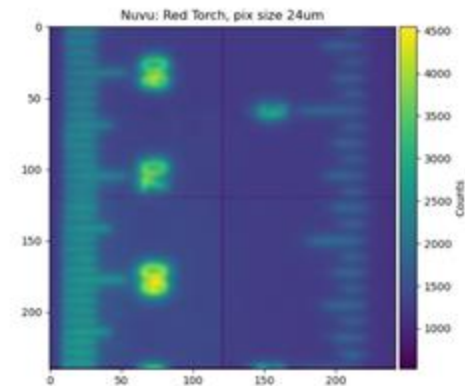
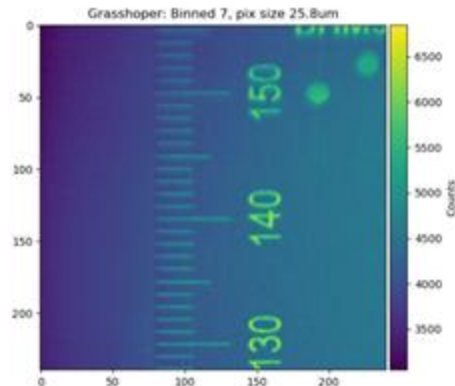
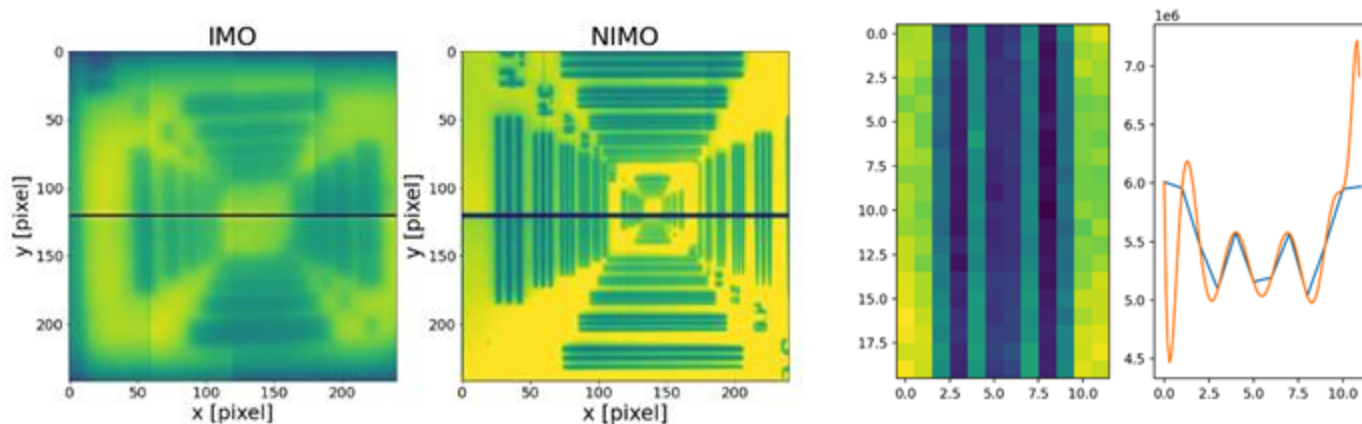


Image Quality Tests

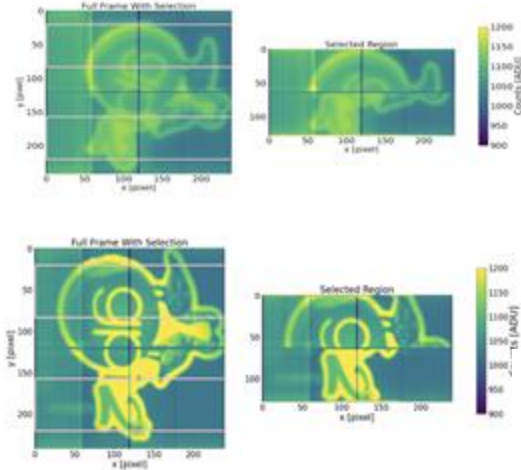
- Camera issue was caused by mode of operations!
- EMCCDs have two modes, **which can be set by the voltage size in the detector**:
 - **Inverted Mode (IMO)**: lower voltage; generates holes in the detector that recombine with dark current (e.g. Downing et al 2015)
 - **Non-Inverted Mode (NIMO)**: higher voltage; potential barrier between adjacent pixels is increased but dark current is increased
- Charge Diffusion Solution: send camera back to Nuvu to change **from IMO to NIMO**



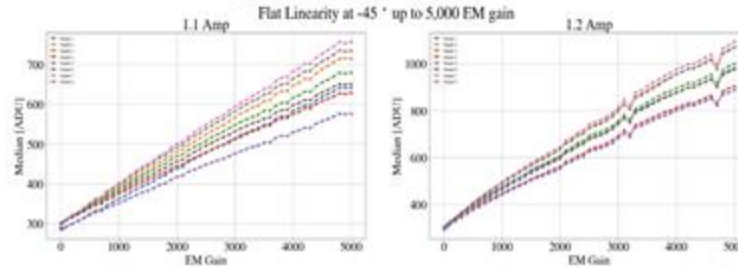
(Do Ó et al in prep)

The EMCCD: Characterization (Do Ó et al 2023 - IMO and Do Ó et al 2024 - NIMO)

Regions of Interest



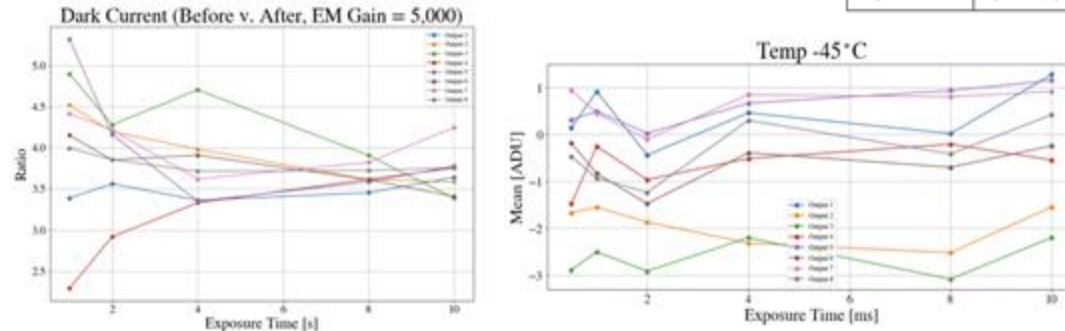
EM Gain Linearity



Readout Noise

Output	IMO (Before)	NIMO (After)
1	0.169787	0.166559
2	0.167197	0.168746
3	0.139553	0.141459
4	0.150889	0.145825
5	0.132648	0.132513
6	0.103851	0.103713
7	0.071985	0.0746640
8	0.127600	0.125917

Dark Current

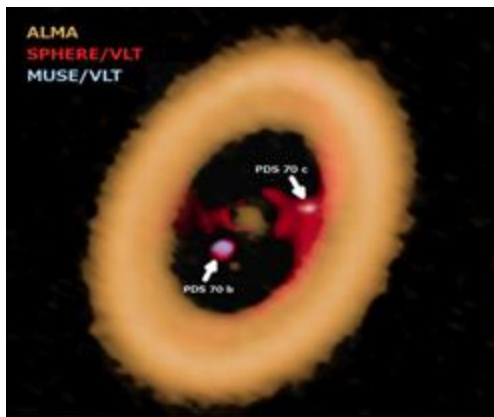
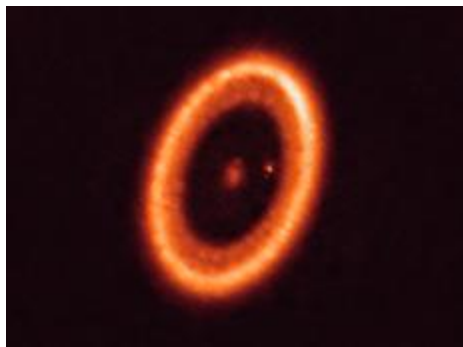




Computational Approach

Protoplanetary Disks

- Mainly made of gas + dust & have an accreting protostar
- Example: **PDS 70 disk (disk + 2 embedded protoplanets!)**
- **What is PDS 70's future?**



Credit: Benisty et al. 2019

System Age	5.4 Myr
Mass	0.76 Msol (star); 7 Mj (PDS 70 b); 4.4 Mj (PDS 70 c)
Period	~ 100 yr (b) & ~200 yr (c)
Eccentricity	0.17 (b) & 0.03 (c)

Muller et al. 2018; Keppler et al. 2018; Stolker et al. 2020

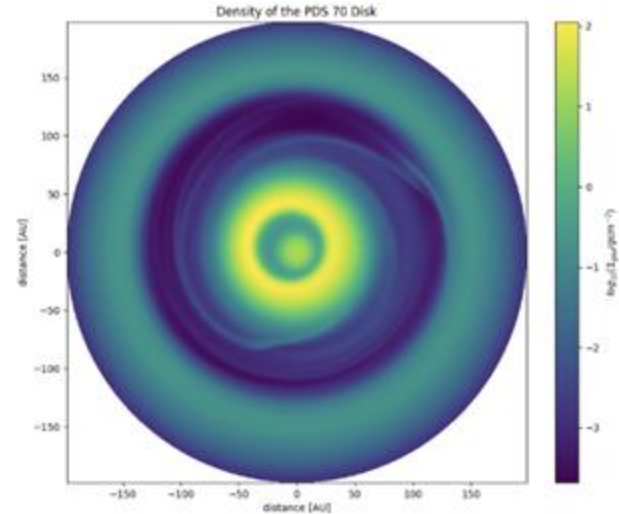
Hydrodynamic Simulations: Disk Evolution

- Since planets are embedded in gas disk, need to simulate dynamics using a hydrodynamic code, such as FARGO3D
- Surface density of the PDS 70 disk as a function of radius (Keppler et al 2018 from radiative transfer models & observations):

$$\Sigma_{gas,init}(R) = \Sigma_c \left(\frac{R}{R_c} \right)^{-1} \exp\left(\frac{-R}{R_c} \right)$$

$$R_c = 40 \text{ au and } \Sigma_c = 2.7 \text{ g cm}^{-2}$$

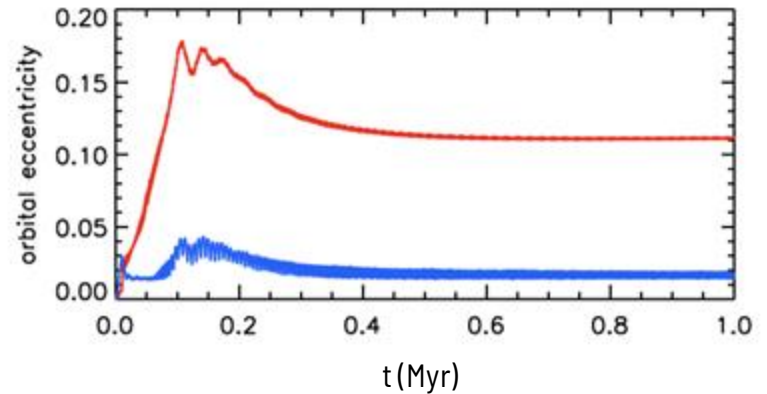
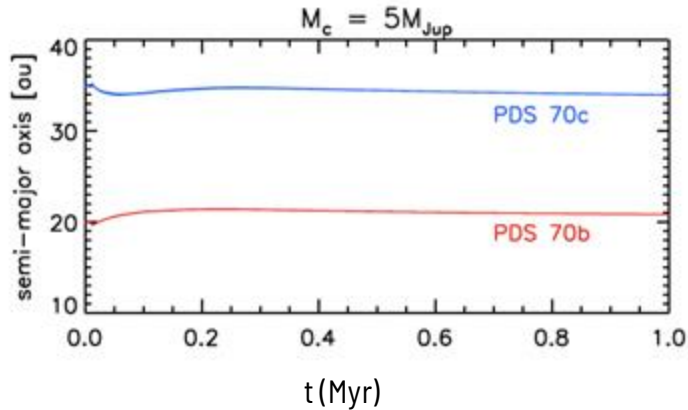
- **Protoplanetary disks go through photoevaporation (dispersion by stellar wind and heating) due to radiation**
- Will analyze what happens to planets once disk evaporates



(Do Ó project from
Protoplanet Disk
class)

Hydrodynamic Simulations: Embedded Protoplanets

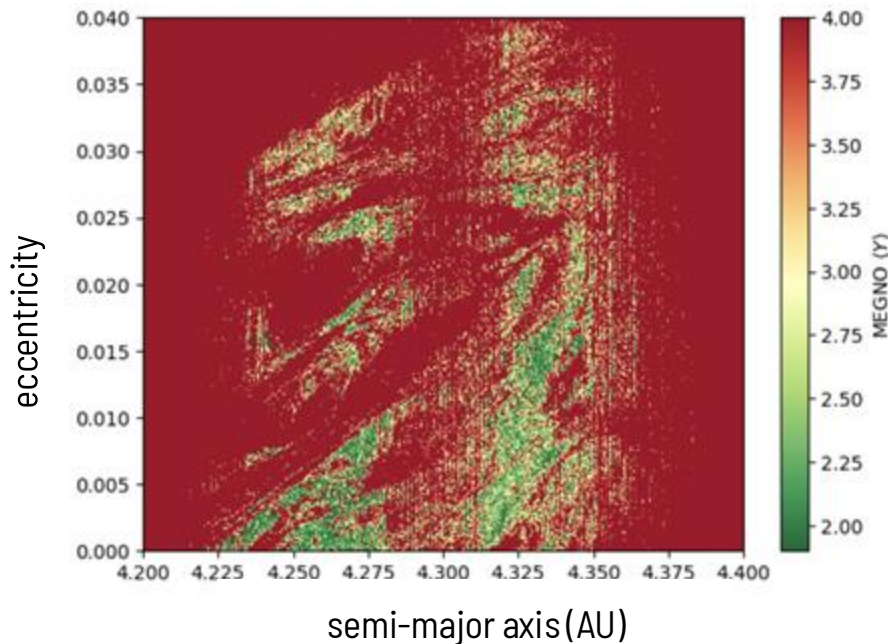
- FARGO3D allows to place embedded protoplanets on disk
- Can input planets' parameters and see how they evolve over time



Credit: Bae et al. 2019

N-Body Simulations

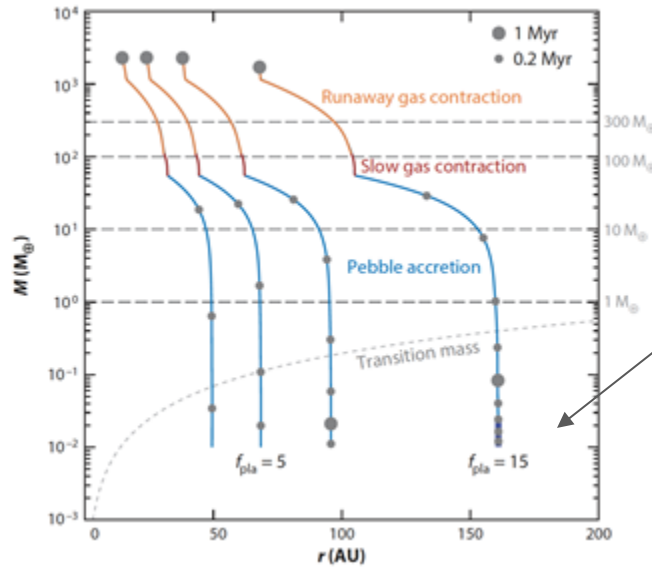
- What happens to planets **once disk is gone?** Instability? MMR?
- Will use N-body integrations to assess stability over time & as a function of orbital parameters



Example plot: stability grid of semi-major axis v. eccentricity for HR 8799 f, a tentative candidate in the HR 8799 system.
(Credit: Thompson et al. 2022)

Core Accretion & Limitations

- Core accretion has **difficulty forming planets beyond 35 AU** (Dodson-Robinson 2009) & timescales that were way too long to explain some directly imaged planets
- **Pebble Accretion** (Lambrechts & Johansen 2012) is a newer form of core accretion that has planetesimals forming from accreting pebbles

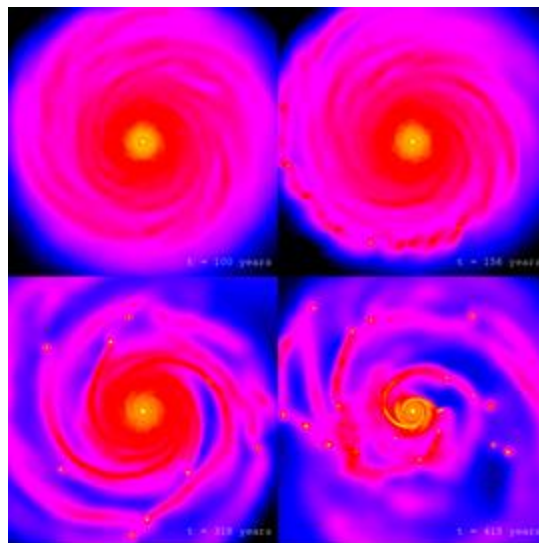


HR 8799 b required
15x the nominal
planetesimal density
to be formed

Johansen & Lambrechts
2017

Gravitational Instability & Limitations

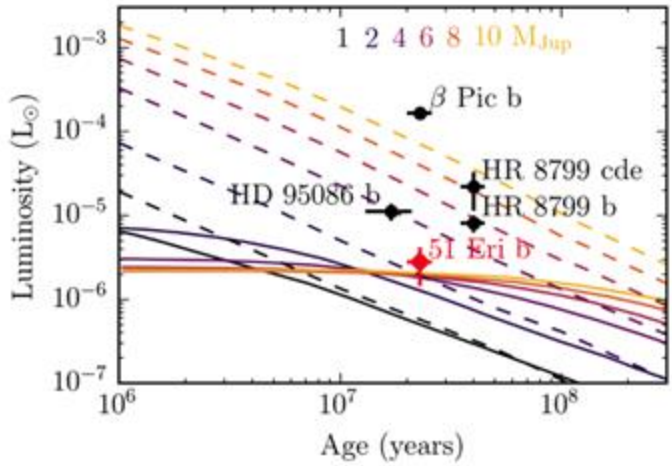
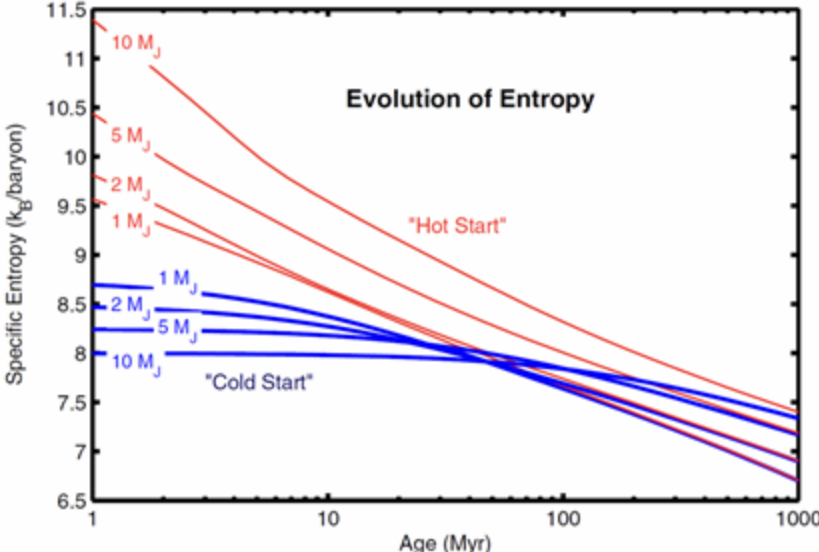
- Forms planets on wide orbits more efficiently than core/pebble accretion
- Difficult to form planets within 40 AU according to simulations (Dodson-Robinson et al. 2009)
- Difficult to make fragments stable (Mejia et al. 2005)



G. Lufkin et al. 2004

Entropy & Formation (Chilcote et al 2018; Spiegel & Burrows 2012)

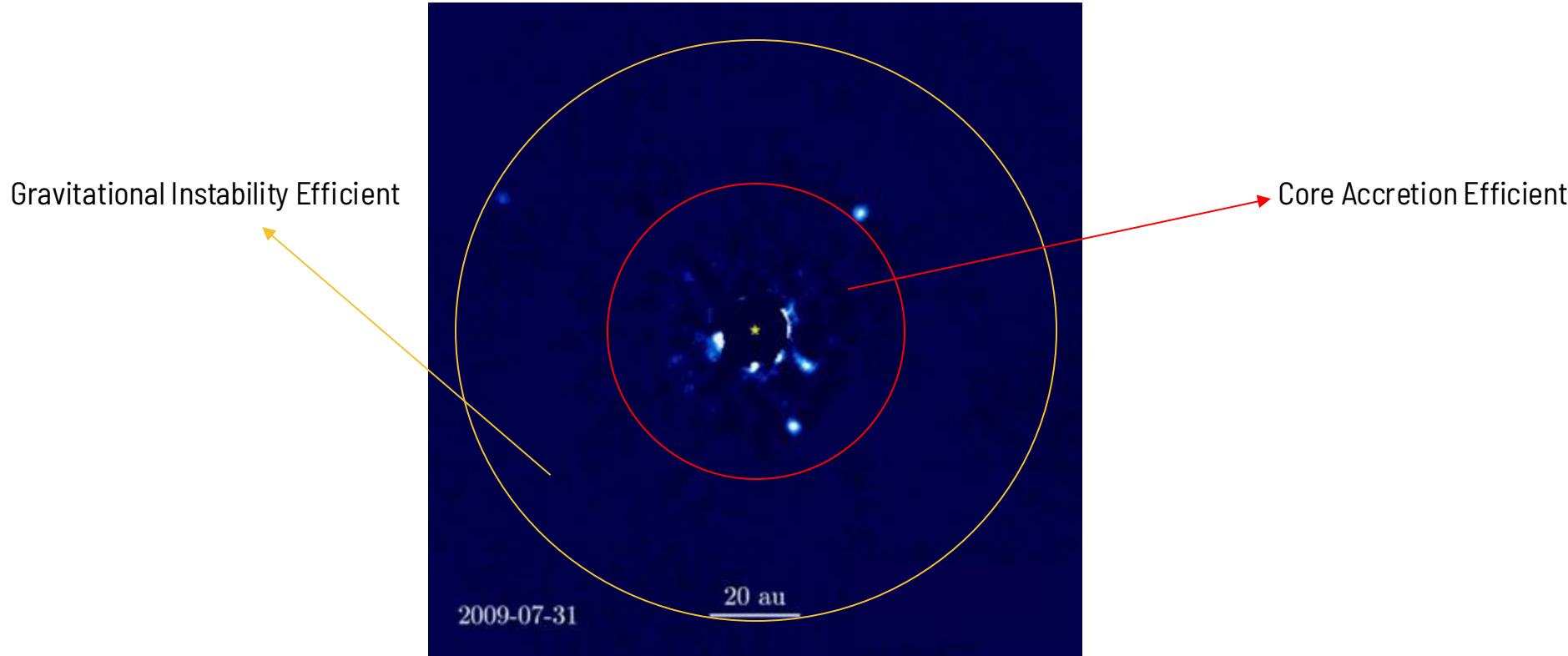
In first few million years after formation, giant planets that started hot can be ~10 to 1,000x more luminous than those that started cold depending on the giant planet's mass and spectral band.



Core accretion: the solid core accretes gas through an accretion disk. This process cools the gas, causing it to lose much of its initial entropy and forms a giant planet that has low initial entropy

Gravitational Instability: the gas that collapses directly to form a giant planet retains most of its initial entropy, resulting in high initial entropy (i.e. a "hot-start").

how did HR 8799 form...?

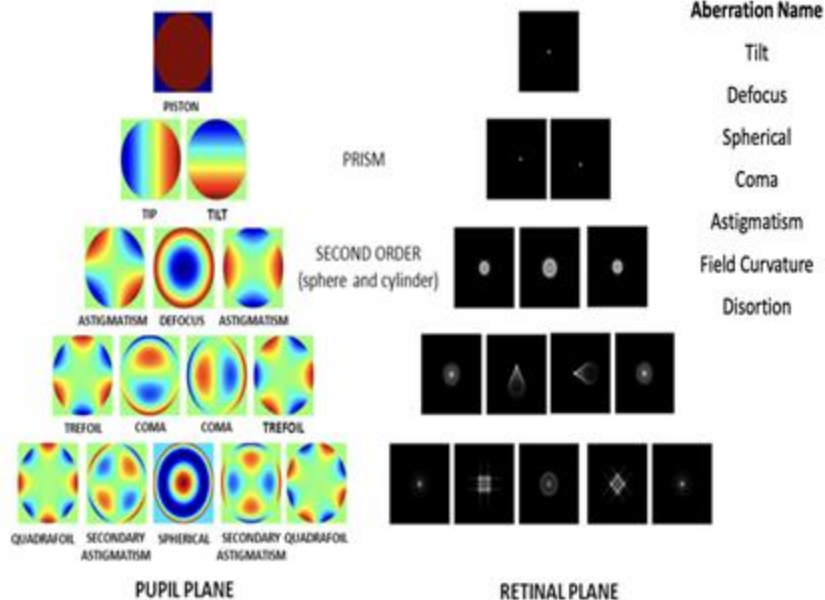
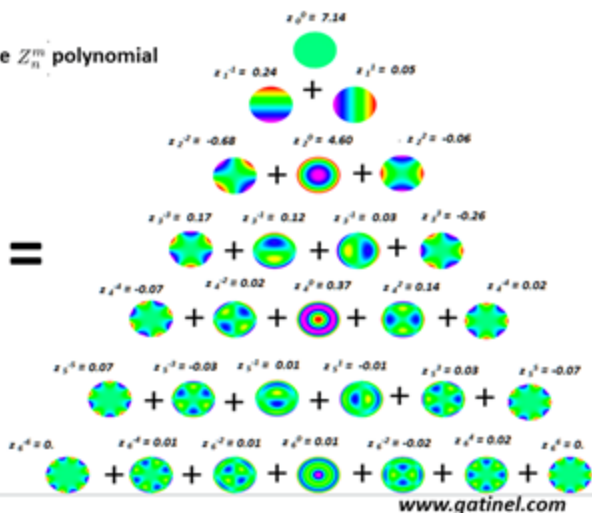
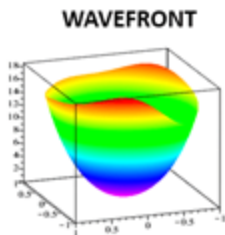


Adaptive Optics: Zernike Polynomials

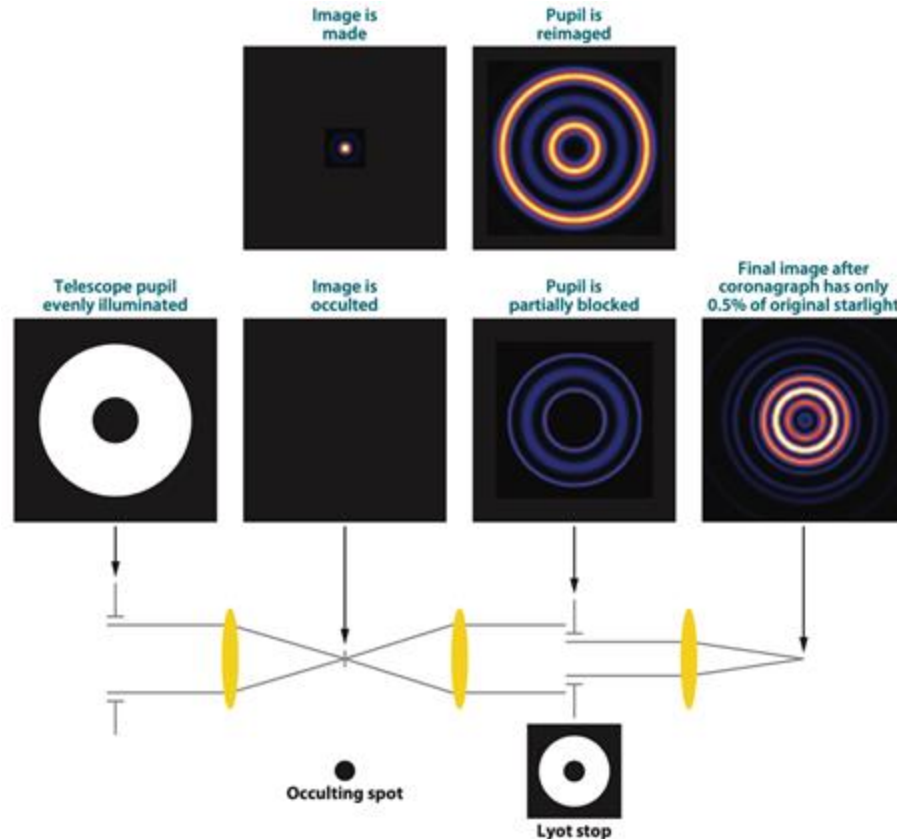
WAVEFRONT ERROR DECOMPOSITION INTO ZERNIKE POLYNOMIALS

$$f = \sum_{n \in \mathbb{N}} \left(\sum_{m \in I_n} z_n^m(f) Z_n^m \right) = \sum_{m \in \mathbb{Z}} \left(\sum_{n \in J_m} z_n^m(f) Z_n^m \right)$$

Coefficient of the Z_n^m polynomial



Lyot Stop Coronagraph (example from MIRI on JWST)



Readout & Dark Noise

Electrons are transferred to amplifier (i.e. a capacitor)



Voltage induced by electron charges is measured by amplifier



Voltage is converted to a number when passed from hardware to computer and turned into a pixel value

Dark current noise is a thermal effect where small currents are generated by electrons on the chip. It can be mitigated by cooling the detector.

Readout noise occurs here. Amplifier can't perfectly measure electron charge every time so there's small variations in electron measurements even where electron counts should be the same from frame to frame

The EMCCD: Test Results

Readout Noise over 1,000 frames: 3k FPS, EM gain 5000 (@ -35 °C)

Output	Median Readout Noise (e-)
1	0.19
2	0.21
3	0.19
4	0.18
5	0.14
6	0.12
7	0.09
8	0.14

EMCCD

- Has additional circuitry to amplify electron signal **BEFORE** readout amplifier - bypasses readout noise while keeping the readout speed high
- Extra register is what induced the "EM Gain" feature in EMCCDs
- Uses impact ionization (captured electrons collide with the multiplication registers' silicon atoms, ripping an electron from the atom. New electron then becomes part of the measured signal)

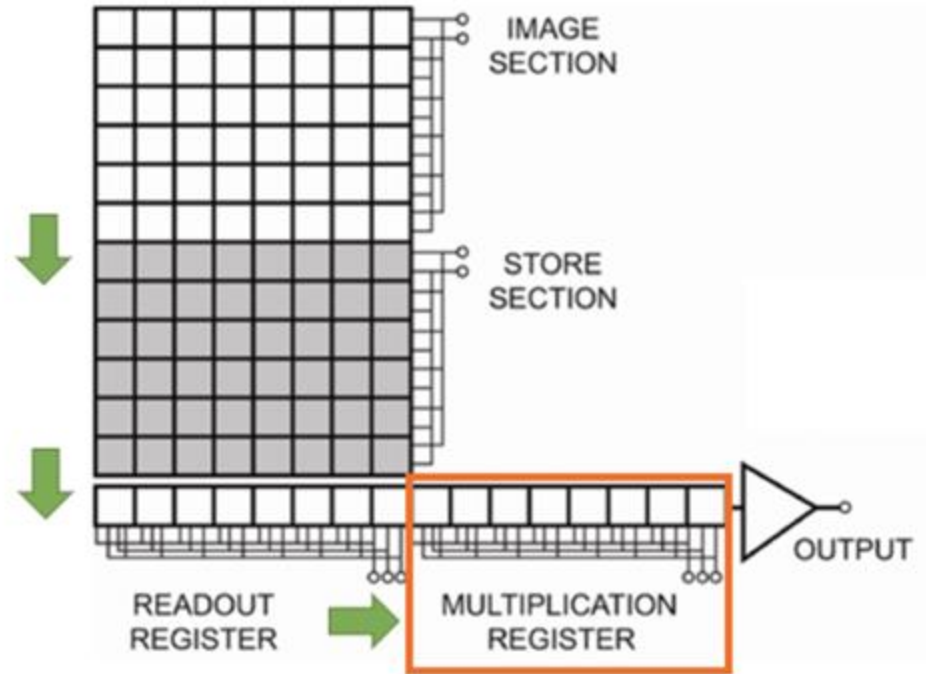
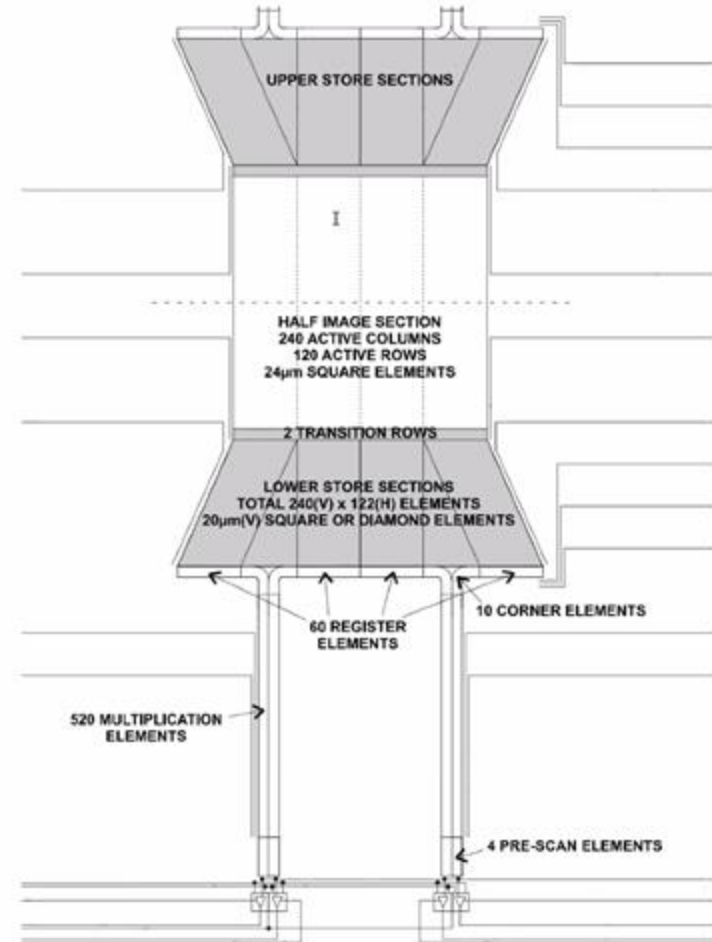


Image: Andor Technologies

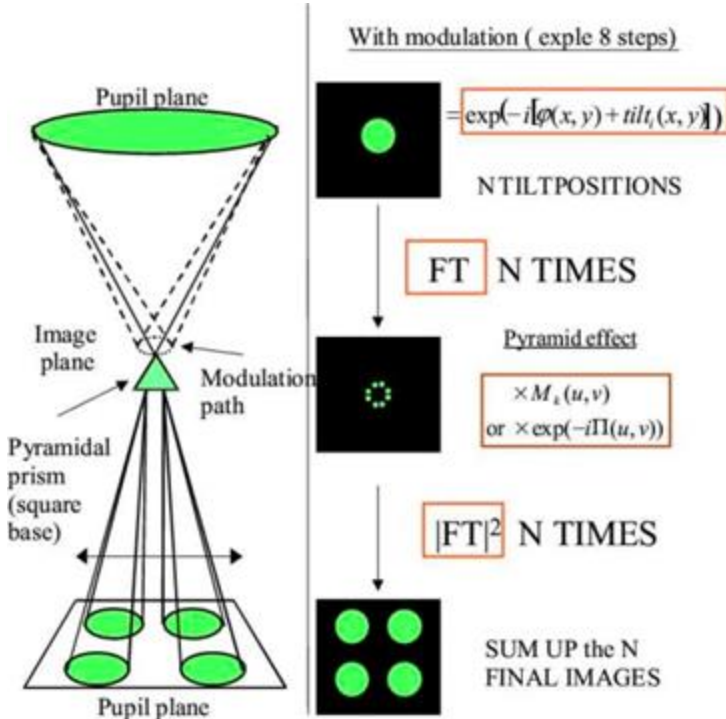
EMCCD

System overview

- Based on the CCD220
 - Split-frame transfer architecture
 - 8 outputs (60x120 pixels per output)
 - EM-only outputs (no Conventional outputs)
- 30MHz pixel read-out frequency
 - 14 bits per pixel
- 10MHz parallel shifting frequency
- 3020 fps (full frame read-out + 1 overscan line)

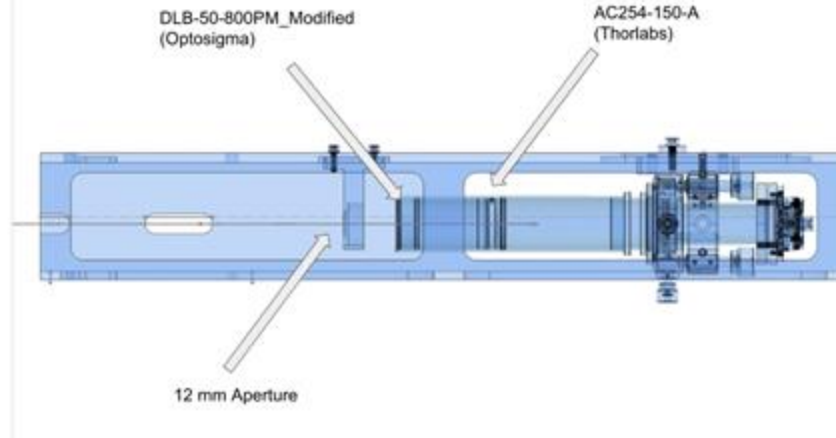
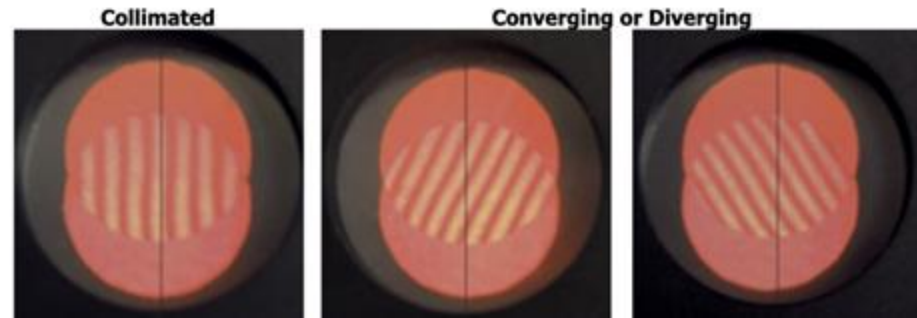
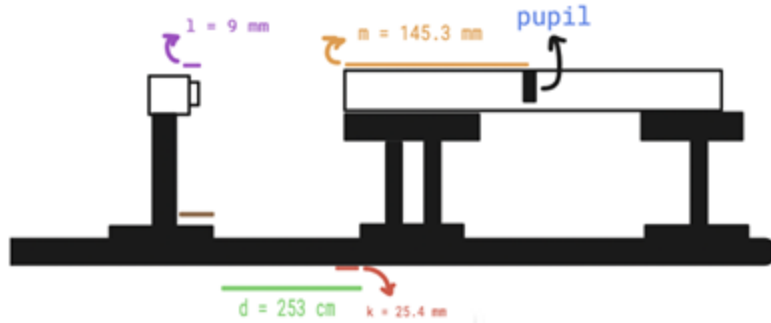


Fast Steering Mirrors & Modulation

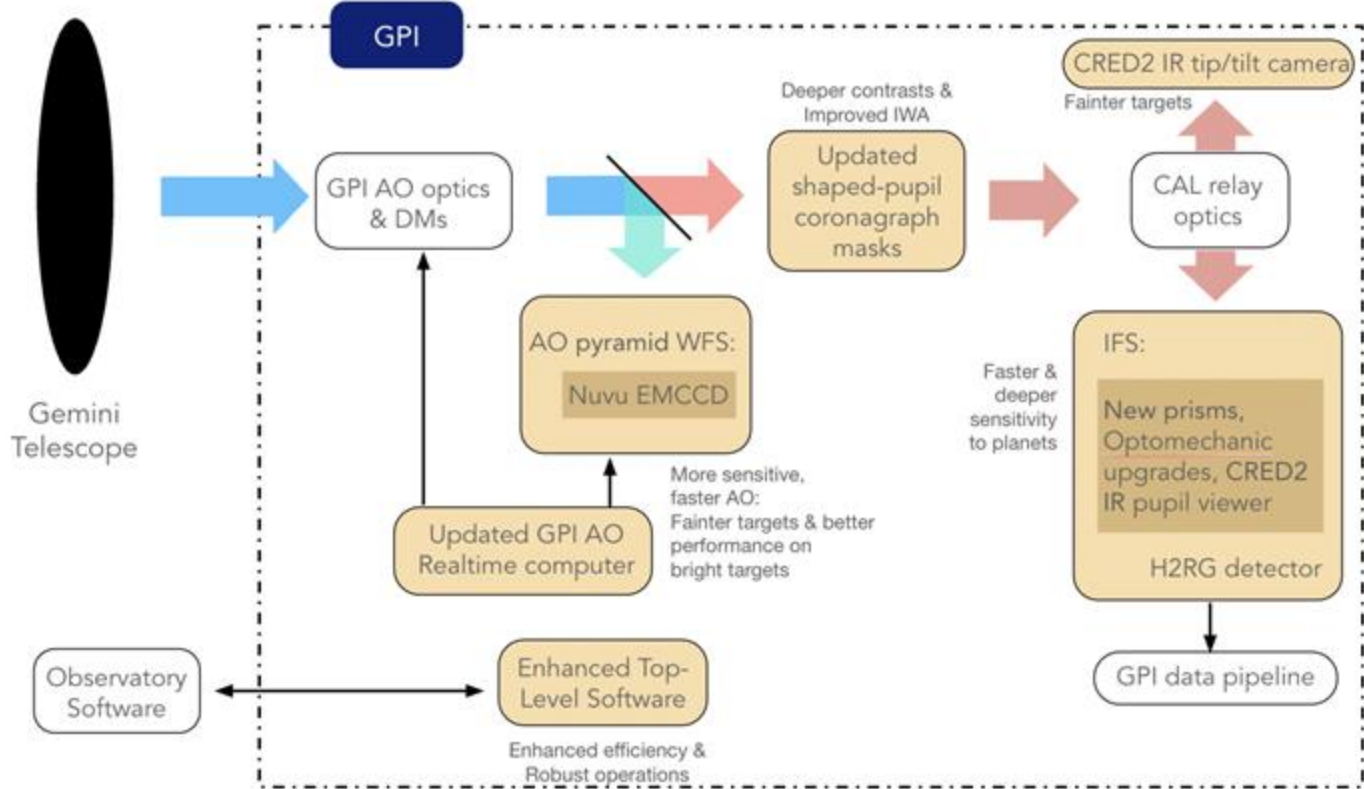


Modulation occurs for averaging purposes and to make sure that the ray spends an equal fraction of the total time on every face of the pyramid

The TSU

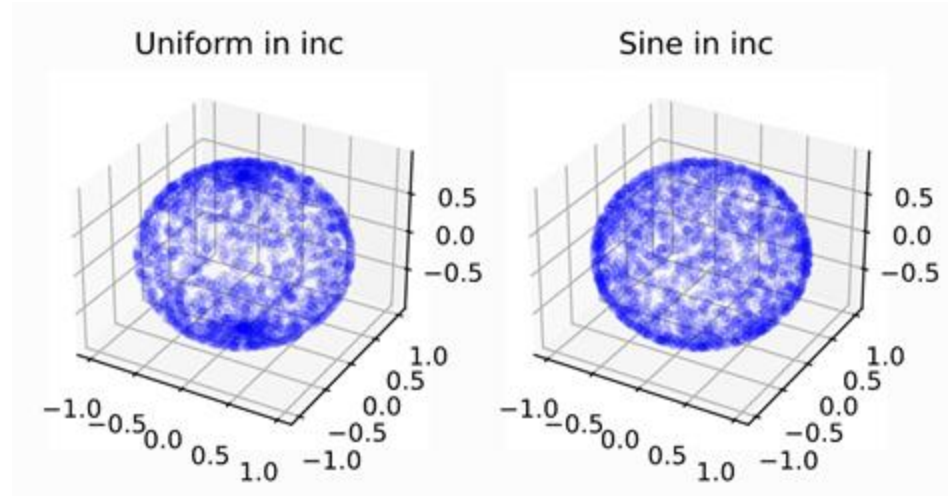
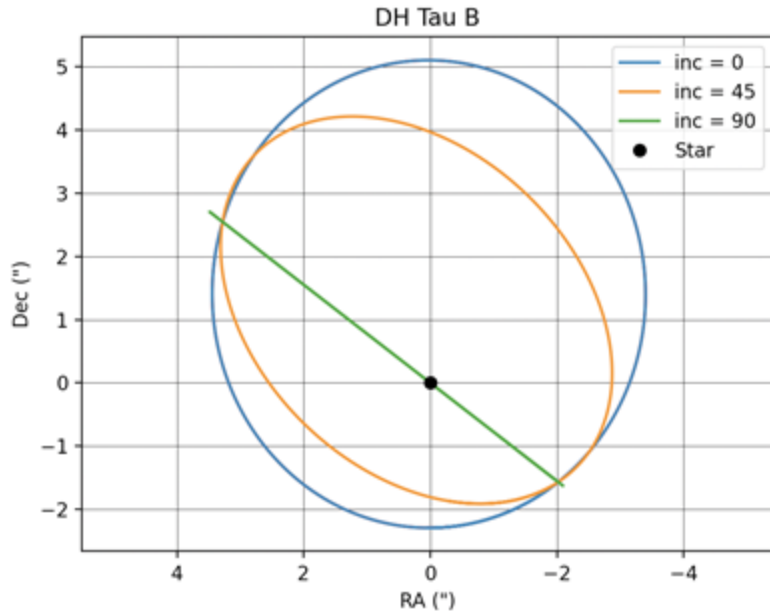


GPI 2.0 Upgrades



Inclination and Sine Prior

- All inclinations should be considered equally likely, but inclinations are not isotropically distributed due to spherical projection on the sky



Orbit Fitting: A step-by-step

Obtain astrometry as a function of time for object



Calculate mean and eccentric anomaly for orbital parameters (both time dependent) using Newton's Method



Relate values to Thiele-Innes constants and find matching $\Delta\delta$ and $\Delta\alpha$ that could be given by data (i.e. compare these to data)

$$\Delta\delta = AX(t) + FY(t),$$

$$\Delta\alpha = BX(t) + GY(t),$$

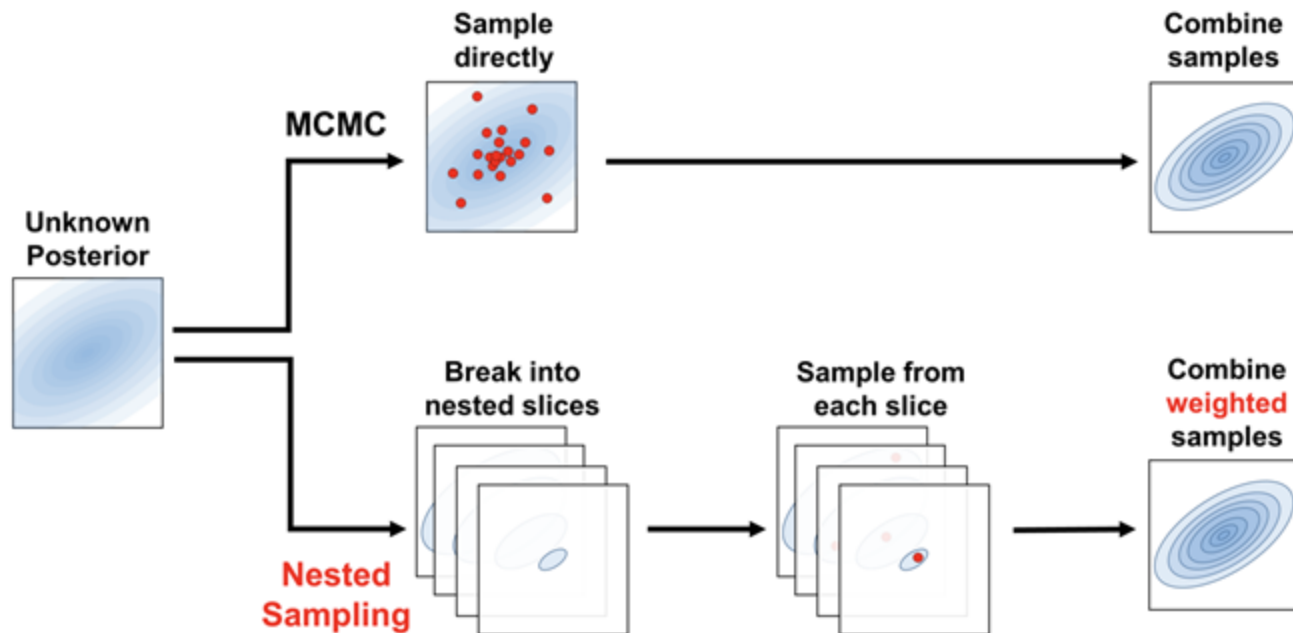
$$\mathcal{L}(\text{Model}) = p(\text{Data}|\text{Model}) \propto \exp\left(-\frac{\chi^2}{2}\right),$$

$$\chi^2 = \sum_i \frac{(\text{Model}_i - \text{Data}_i)^2}{\sigma_i^2}$$

Mede & Brandt 2016

We can find the posterior distributions by finding the likelihood of model * prior model for **all parameter combinations**, but in our case Keplerian orbits have a 6 dimensional parameter space! We need samplers!!

MCMC vs. Nested Sampling



Newton's Method & Eccentric Anomaly

Measures where body currently is in its orbit. Can't solve for eccentric anomaly using Kepler's equation analytically:

$$E - e \sin E = 2\pi/P (t - T_0)$$

We can use Newton's Method which iterates guesses on E (here represented by X) until its change is small enough such that it approaches a value that solves Kepler's equation (we set eps. to floating-point precision of $\sim 1e-15$)

```
X ← initial guess  
repeat  
     $dX \leftarrow -f(X)/f'(X)$   
     $X \leftarrow X + dX$   
until  $|dX/X| < eps.$ 
```

Maximum Likelihood Estimation

- Aims to find the parameters of a model

Define model (here,
Beta distribution)



Find Derivative of the
logarithm of model
(e.g., with respect to
alpha/beta, setting x
values = to posteriors)



Set derivative = 0 to
obtain maxima (and
minima) of function

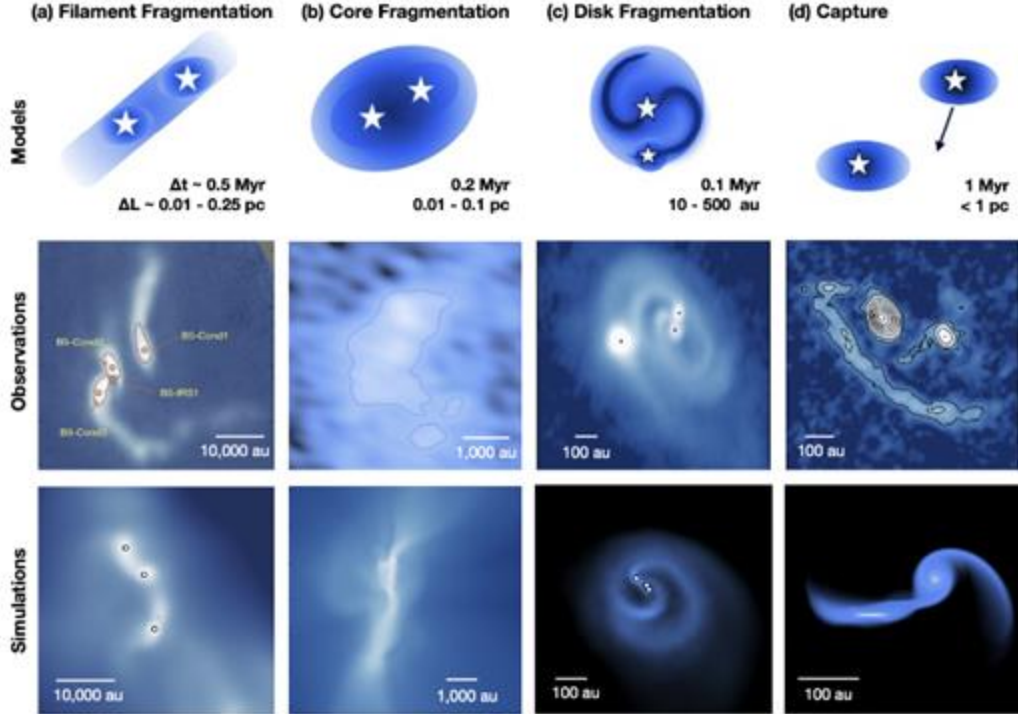
$$f(e, \alpha, \beta) = \frac{\Gamma(\alpha + \beta)e^{\alpha-1}(1 - e)^{\beta-1}}{\Gamma(\alpha)\Gamma(\beta)}$$

Orbital Parameters & Priors

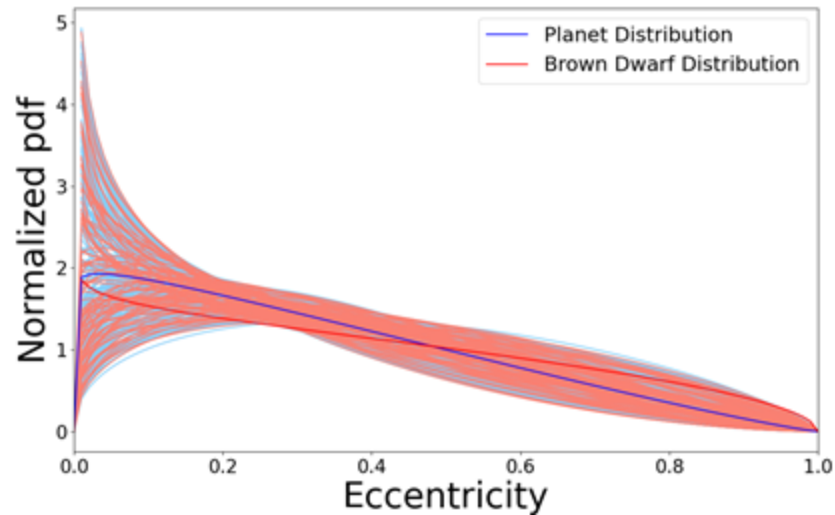
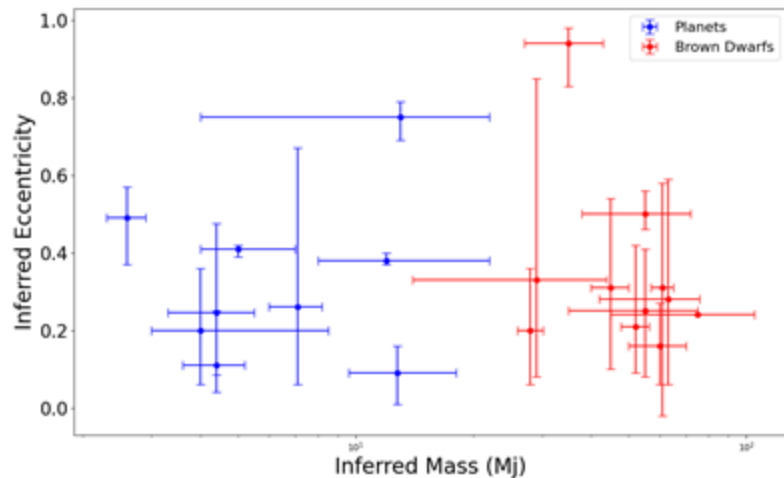
Orbital Parameter	Name	Range and Unit	Generally Used Priors
P	Period	Dependent on separation (Years)	Log-Uniform
e	Eccentricity	0 to 1 (Unitless)	Uniform
i	Inclination	0 to 180°	Sine
Ω	Longitude of the ascending node	0 to 360°	Uniform
ω	Argument of periapsis	0 to 360°	Uniform
T_o	Epoch of periapsis passage	Dependent on separation (Years)	Uniform

NOTE—One can switch from period to semi-major axis using Kepler's Third Law and the total system mass.

Binary Star Formation v. Planet Formation

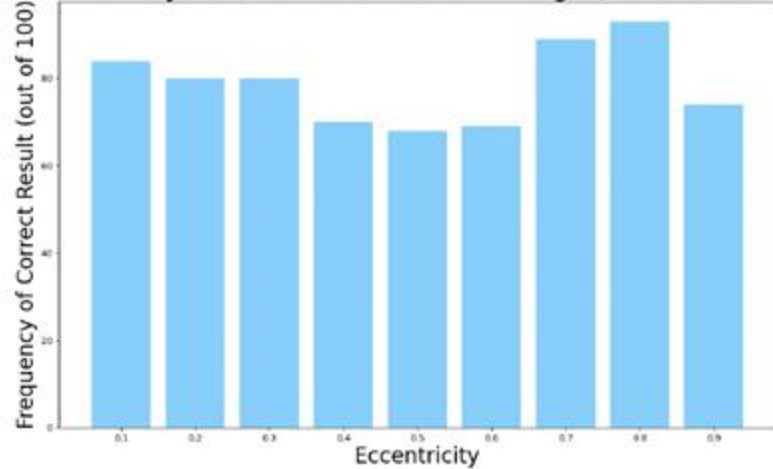


More results on orbit fitting...

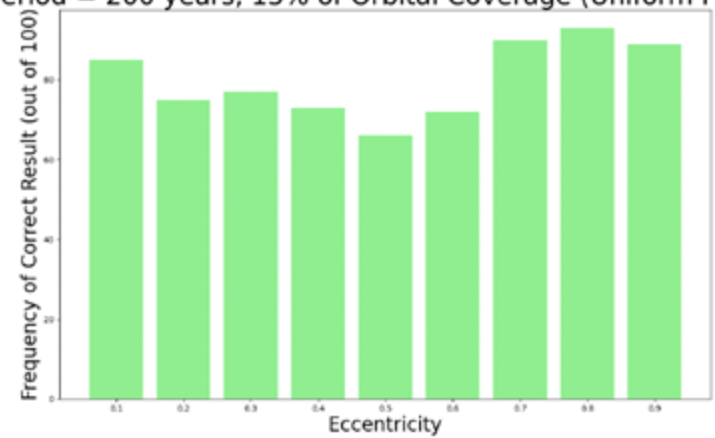


More results on orbit fitting...

Period = 200 years, 15% of Orbital Coverage (Observable Priors)

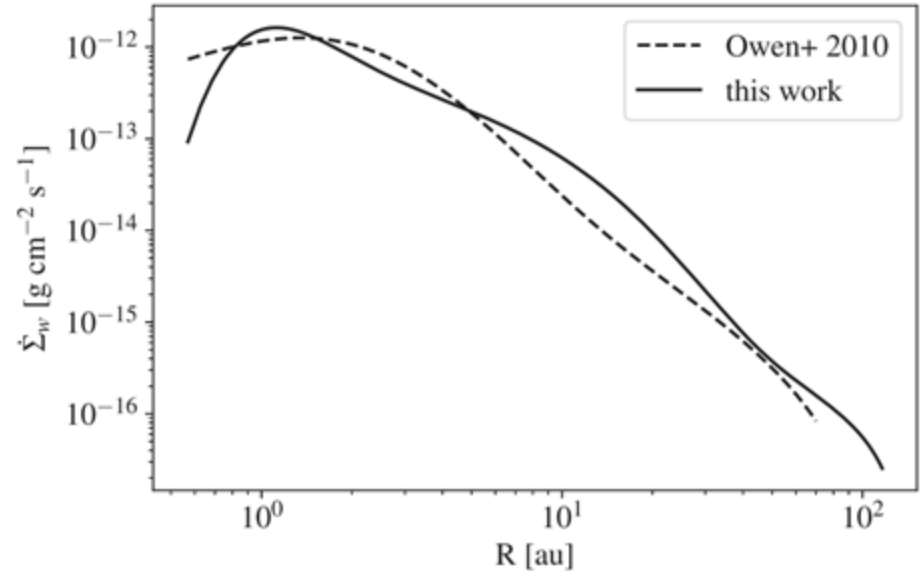


Period = 200 years, 15% of Orbital Coverage (Uniform Priors)



Photoevaporation of Disks (Picogna et al. 2019)

- Protoplanetary disks go through photoevaporation (dispersion by stellar wind and heating) due to radiation
- Explore the dependence of the wind mass-loss rates on stellar X-ray luminosity
- Use temperature parametrizations from detailed radiative transfer calculations that solve the heating and cooling equations



Photoevaporation Prescription

- From radiative transfer models for a 0.7 Msol star

$$\dot{\Sigma}_w(R) = \ln(10) \left(\frac{6*a*\ln(R)^5}{R*\ln(10)^6} + \frac{5*b*\ln(R)^4}{R*\ln(10)^5} + \frac{4*c*\ln(R)^3}{R*\ln(10)^4} + \frac{3*d*\ln(R)^2}{R*\ln(10)^3} + \frac{2*e*\ln(R)}{R*\ln(10)^2} + \frac{f}{R*\ln(10)} \right) \frac{\dot{M}_w(R)}{2\pi R} [M_\odot au^{-2} yr^{-1}]$$

a = -0.5885, b = 4.3130, c: -12.1214, d = 16.3587, e = -11.4721, f = 5.7248, g = -2.8562 (Picogna et al. 2019)

N-Body Integration

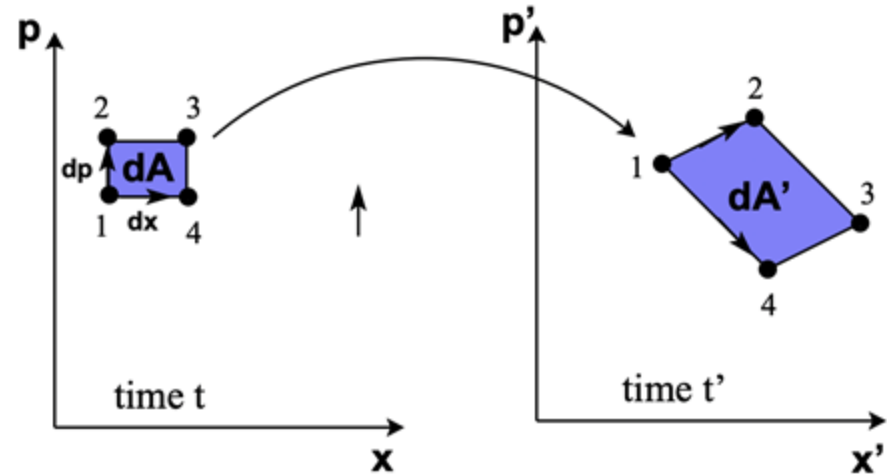
- Aims to see how n-bodies interact with each other gravitationally (using for instance Newton's second law):

$$\vec{F}_i = - \sum_{j \neq i} G \frac{m_i m_j (\vec{r}_i - \vec{r}_j)}{|\vec{r}_i - \vec{r}_j|^3}, \quad \frac{d^2 \vec{r}_i}{dt^2} = \vec{F}_i / m_i.$$

- Numerically solve for a second order differential equation; it's a balancing game of higher accuracy (for smaller timesteps) & computational time (infinitely small time step would take forever)

Symplectic vs. Non-symplectic Integrators

- Symplectic integrators preserve area in phase space
 - Energy is not quite conserved, but it is bounded
 - Likely more reliable for long term integrations
 - **Limitation: not great when non-conservative forces are at play, including radiation forces in a protoplanetary disk (e.g. Rein & Spiegel 2015)**
- Non-symplectic integrators turn a conservative system into a dissipative one
 - Require less functions & can use larger timesteps to produce accurate results for short term integrations
 - Easier to implement adaptive step sizes

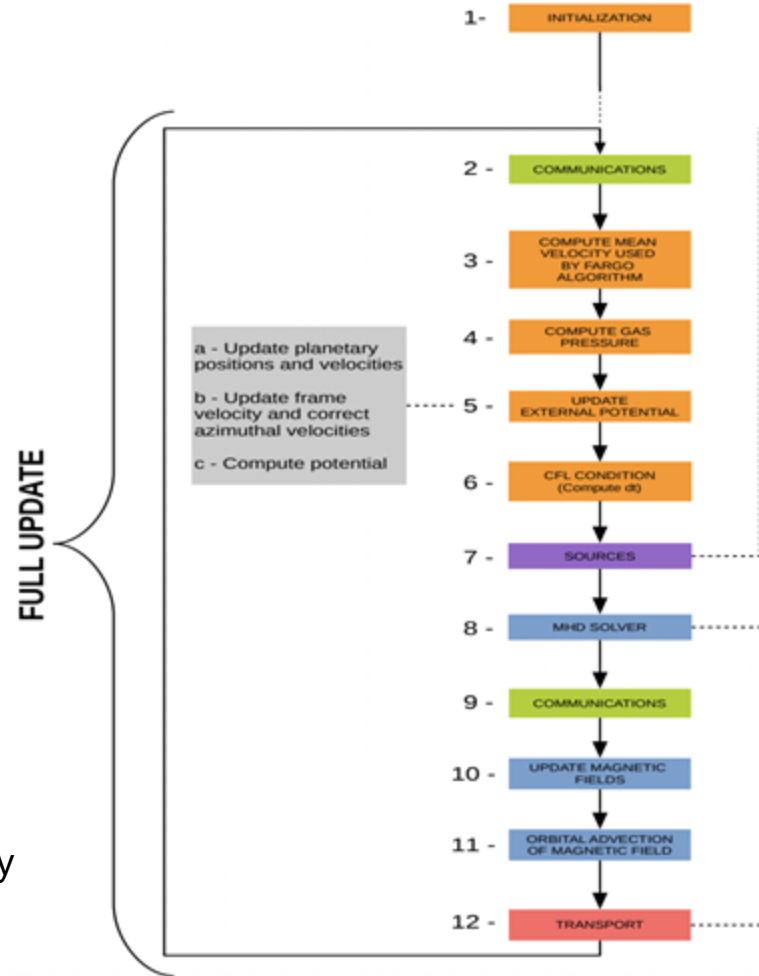


Young 2014

FARGO3D's N-Body Integrator

- Runge-Kutta method
5th order integrator w/
Cash-Karp method
(non-symplectic)
- Fixed timestep based
on Courant-Friedrichs-
Lewy (CFL) condition
which here is that
information cannot
travel over more than
one gas cell per step
- Possible to switch
integrator if needed (if
close encounters
occur)

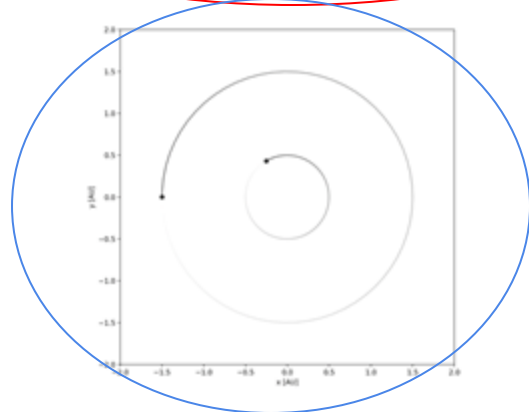
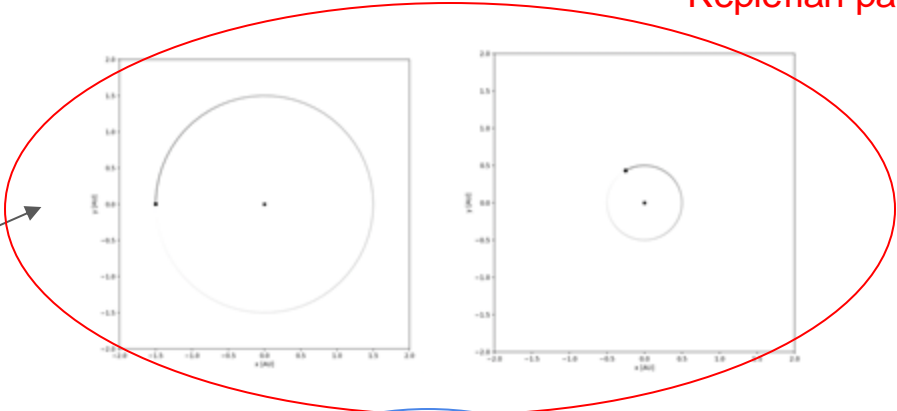
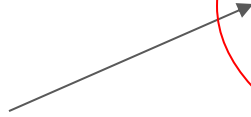
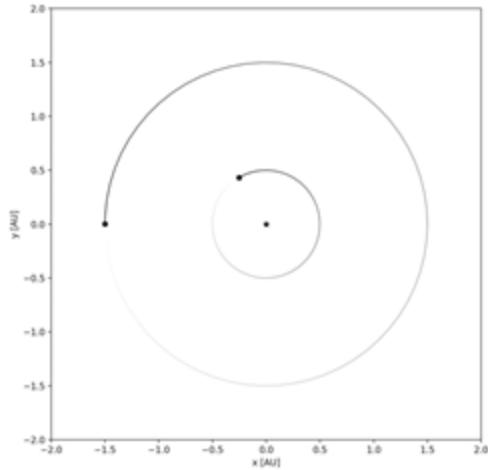
Benitez-Llambay
2015



WHFast Integrator

Based on Wisdom & Holman 1991; from Rein & Tamayo 2015

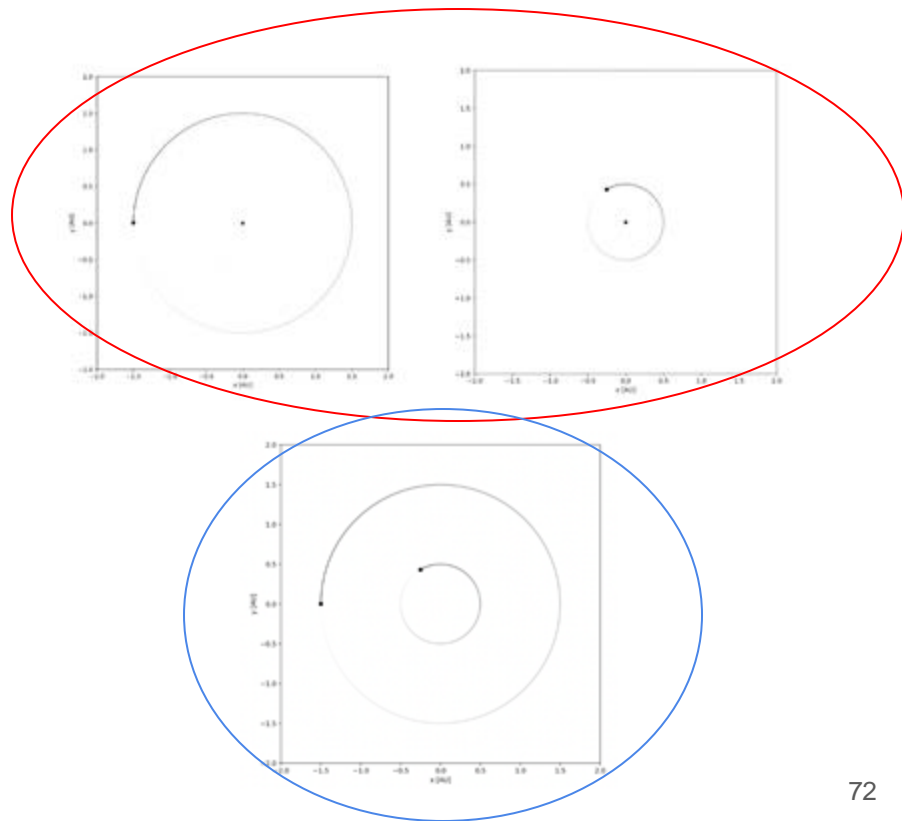
Keplerian part



Interaction Part

WHFast Integrator - Timestep evolution

- Evolve particles for 0.5 a timestep assuming Keplerian Orbits
- Calculate gravitational acceleration from planet-planet interaction and update velocity for a full timestep
- Update particle positions for another 0.5 time step assuming Keplerian orbits
- Default: 11th order integration




(slide based on Hanno Rein's WHFast talk)

Integration & MEGNO (from Rein & Tamayo 2015)

- Idea: introduce shadow particle which is slightly perturbed from true particle and see whether its trajectory diverges from true particle's trajectory in phase space (position vs. momentum space)
 - Unstable systems will have these trajectories exponentially diverging so MEGNO $\rightarrow \infty$
 - Stable systems have MEGNO converging to value of 2

$$\boldsymbol{\xi}_i^S = \boldsymbol{\xi}_i + \boldsymbol{\delta}_i;$$

Displacement
vector



$$Y(t) = \frac{2}{t} \int_0^t t' \frac{\sum_{i=0}^{N-1} \dot{\boldsymbol{\delta}}_i(t') \cdot \boldsymbol{\delta}_i(t')}{\sum_{i=0}^{N-1} \boldsymbol{\delta}_i^2(t')} dt'.$$

Migration Type I

- For less massive planets, where surface density of disk is not strongly affected by planet's gravity
- Interaction with **interior of disk adds angular momentum to planet while with exterior of disk removes angular momentum from planet**. Inner/outer migration will depend on which of these effects wins

Migration Type II

- More massive planets really perturb disk
- Tidal torque around planet causes a gap to surround the planet in the disk
- Planet excites density waves
- Possible explanation for how hot Jupiters formed
- Whether planet migrates in or out depends on planet's location

Tonight's observing specs !

Table 1: Target Properties for 2023A

Planet Name	Planet Estimated Mass (M_{Jup})	Sep. (")	Estimated Period (yrs)	Estimated Eccentricity	Current Phase Coverage	Coverage with new 23A data
1RXS0342+1216 B	35	0.8	232	0.93	4.7%	6.9%
DH Tau B	11	2.4	13500	0.38	0.1%	0.2%
HD 49197 B	63	0.9	250	0.28	6.5%	8.5%